RM E53L15b

RESEARCH MEMORANDUM

PRELIMINARY INVESTIGATION OF SEVERAL TARGET-TYPE THRUST-REVERSAL DEVICES

By Fred W. Steffen, H. George Krull, and Carl C. Ciepluch

Lewis Flight Propulsion Laboratory
Cleveland, Ohio

NATIONAL ADVISORY COMMITTEE
FOR AERONAUTICS

WASHINGTON
March 12, 1954

NATIONAL ADVISORY COMMITTEE FOR AERONAUTICS

RESEARCH MEMORANDUM

PRELIMINARY INVESTIGATION OF SEVERAL TARGET-TYPE THRUST-REVERSAL DEVICES

By Fred W. Steffen, H. George Krull, and Carl C. Ciepluch

SUMMARY

Thrust-reversal performance of several basic target-type jet deflectors of various sizes and with various modifications was obtained with unheated air over a range of exhaust-nozzle pressure ratios from 1.7 to 3.0. Reversed thrusts up to 58 percent were achieved.

Maximum, or near maximum, reversal for any deflector occurred at a spacing which was mechanically feasible and which did not affect nozzle air flow.

Two easily retractable deflectors, a simple hemisphere and a double-skin hemisphere, the latter designed to control reversed jet direction, were investigated while installed on a model of a turbojet engine tail pipe and cowling assembly. Reversal produced by the installation with either deflector was found to be about 40 percent at a nozzle pressure ratio of 2.0. With the simple hemisphere, 50 percent of the available thrust was lost through insufficient turning and 11 percent was lost through air-flow reduction, shock, and friction.

INTRODUCTION

Modern jet aircraft, having high wing loadings and attendant high landing speeds, require an effective braking device to safely accomplish landings within the distances allowed by present-day airports. Three methods of braking jet aircraft are now in common use; wheel braking, drag parachute braking, and arrester gear braking. The analysis of reference 1 has shown that wheel braking is generally inadequate and is heavily dependent upon runway surface conditions and that drag parachute

braking requires high initial deceleration to materially affect the landing distance. Arrester gear braking, of course, requires that the equipment and attending personnel be present at all landing fields from which the aircraft is to be operated.

A fourth method, thrust reversal, also analyzed in reference 1, could provide throttle-controlled deceleration at all speeds under all types of runway conditions without the aid of any ground equipment. Small amounts of thrust reversal have been obtained with target-type thrust spoilers and are reported in reference 2.

Because thrust reversal appears to be the most desirable method of braking military and commercial jet aircraft, the NACA Lewis laboratory has undertaken an experimental investigation to improve the reversal performance of target-type jet deflectors and to determine some of the factors which affect thrust reversal, such as deflector geometry, size, and spacing.

The performance of a small-scale model of a practical thrust-reversal installation and a segregation of the incurred reversal losses were also obtained. The model included a deflector which had shown good reversal characteristics combined with a geometry suitable for retraction and a tail pipe and cowling with space for deflector stowage.

APPARATUS AND PROCEDURE

Equipment and Instrumentation

The mechanism used to measure thrust in both positive and negative directions is shown in figure 1. The air-supply duct was connected to the laboratory air system by flexible bellows and pivoted to a steel frame so that axial thrust forces along the pipe, both forward and reverse, could be freely transmitted and directly read from a balanced-pressure diaphragm, null-type, thrust-measuring cell. To assure that the steel strap used to transmit the force from the duct to the thrust cell was always in tension, it was sometimes necessary to preload the system with counterweights.

The simple exhaust nozzle also shown in figure 1 had a half-cone angle of 8°, an exit diameter of 4 inches, and a 5-inch-outside-diameter approach pipe. The deflectors were mounted on four rods extending from tabs located 8 inches ahead of the exhaust-nozzle exit.

Exhaust-nozzle air flow was measured by means of a standard A.S.M.E. sharp-edged orifice. Two total-pressure tubes, about 8 inches ahead of the exhaust-nozzle exit, were used to measure exhaust-nozzle inlet pressure, while a barometer was used to measure ambient exhaust pressure.

Figure 2 shows the model engine tail pipe and cowling mounted on the air supply duct. The exhaust nozzle on this configuration had a 6.3° half angle and a 4-inch exit diameter. Other dimensions were scaled down from a typical nacelle-type turbojet engine installation.

Instrumentation for the configuration shown in figure 2 was similar to that of the simple exhaust nozzle except for the addition of a total-pressure tap underneath the retraction fairing and a movable pitot-static tube, mounted on the floor of the test cell, which was used to measure the magnitude and direction of the reversed jet.

Deflectors

Typical deflector geometries are shown in figure 3. Table I gives the dimensions and the geometries of the 17 deflectors investigated. The 17 deflectors were composed of four basic configurations, namely the $1\frac{1}{2}$- and 2-diameter single-circular-arc type and the $1\frac{1}{2}$- and 2-diameter double-circular-arc type, in three stages of modification, open end, closed end, and closed and filleted end, and five miscellaneous deflectors. The radii of the fillets added to the four basic configurations were equal to the circular-arc radii of the deflector in which they were installed and all the deflectors except the 2.2-diameter cup and the $1\frac{1}{2}$-diameter hemispheres had square frontal projections.

Procedure

Corrected forward thrusts and air flows of both the simple exhaust nozzle and the model tail pipe and cowl were first determined over a range of exhaust-nozzle pressure ratios from 1.7 to 3.0. The deflectors, with the exception of configuration Q, the double-skin hemisphere, were then in turn attached to the simple exhaust-nozzle installation at various spacings and their performance evaluated over the same range of nozzle pressure ratios.

The reversal provided by a complete thrust-reversal installation over a range of exhaust-nozzle pressure ratios was determined by means of the model tail pipe and cowl and two deflectors, configuration P, the 1.5-diameter hemisphere, and configuration Q, the 1.5-diameter double-skin hemisphere.

For the entire investigation, unheated air was used and the nozzle pressure ratio was regulated by variation of inlet pressure.

RESULTS AND DISCUSSION

Basic Data

Reversal and air-flow ratio over a range of nozzle pressure ratios from 1.7 to 3.0 at various spacings for all the various types and modifications of reversal devices investigated are shown in figure 4. Reversal is defined as the ratio, in percent, of the resultant reverse corrected jet thrust of the exhaust nozzle - deflector assembly at a given exhaust-nozzle pressure ratio to the forward corrected jet thrust of the exhaust nozzle alone at the same given exhaust-nozzle pressure ratio. Air-flow ratio is defined as the ratio, in percent, of the corrected air flow passed by the exhaust nozzle - deflector assembly at a given exhaust-nozzle pressure ratio to the corrected air flow passed by the exhaust nozzle alone at the same given exhaust-nozzle pressure ratio. Deflector spacing is defined as the distance from the exhaust-nozzle exit to the rear face of the deflector. Deflector size and spacing are referred to in terms of exhaust-nozzle diameters.

While most of the important trends in deflector performance are more clearly shown by the use of subsequent cross plots and a summary curve at a particular pressure ratio, the curves in figure 4 are included to present data over a complete range of pressure ratios and spacings for each deflector.

The performance of four basic configurations, namely, the $1\frac{1}{2}$-diameter and 2-diameter single-circular-arc deflectors, and the $1\frac{1}{2}$-diameter and 2-diameter double-circular-arc deflectors are shown in figures 4(a) to 4(d). The performance, at various spacings, of the four basic configurations with the ends closed by the addition of flat plates is shown in figures 4(e) to 4(h). The results obtained with a further modification to the four basic configurations, the addition of fillets, are presented in figures 4(i) to 4(l). Data obtained from four additional configurations, a $1\frac{1}{2}$-diameter double-circular-arc deflector, ends closed and filleted with sides extended, a 1-diameter single-circular-arc deflector with ends closed and filleted, a 2.2-diameter cup-shaped deflector, and a 1.5-diameter hemispherical deflector are shown in figures 4(m) to 4(p).

Variation of Reversal with Nozzle Pressure Ratio

Variation of reversal with nozzle pressure ratio may also be noted from the foregoing curves. Maximum variation in reversal for all configurations, with the exception of the 1.5-diameter hemisphere, amounted to about 10 percentage points over a range of nozzle pressure ratios from 1.7 to 3.0. The variation was considerably less, however, for closed-end configurations at near-optimum spacings. The 1.5-diameter hemisphere, while somewhat more sensitive to pressure ratio than other closed-end configurations, showed extreme sensitivity at some spacings less than optimum, probably because of an instability of reversed jet direction observed at these spacings.

Variation of Reversal with Air Flow

It could be expected that maximum reversal would occur at a spacing just great enough to permit passage of 100 percent of the normal air flow. Any lesser spacing would cause reversal losses through losses in air flow and any greater spacing would cause reversal losses through incomplete turning. That maximum or near-maximum reversal does occur at a spacing which allows an air-flow ratio of 100 percent is shown in figure 5, which is a cross plot of air-flow ratio against reversal, including data from all the foregoing configurations with the exception of the 1-diameter configuration. Consequently, these deflectors can be utilized to their full extent, if properly positioned, without any effect on engine operation.

Variation of Reversal with Deflector Spacing and Deflector Spacing Required for 100 Percent Air-Flow Ratio

The effect of deflector spacing on reversal and the spacing required for 100 percent air-flow ratio at a nozzle pressure ratio of 2.0 are shown in figure 6 for the same configurations. Reversal performance of the open-end configurations is less sensitive to spacing, at spacings which give less than 100 percent air-flow ratio, than are the closed-end configurations. At spacings greater than that required for 100 percent air-flow ratio, reversal performance, for both open-end and closed-end deflectors, is only slightly affected by change in spacing within the range of spacings investigated. The range of spacings required for 100 percent corrected air-flow ratio for these deflectors varies from about 0.66 to 1.3 nozzle diameters. The spacings required for 100 percent air-flow ratio appear, therefore, to be within the limits of mechanical feasibility.

Relative deflector performance as affected by size, geometry, and modification of geometry. - The relative performance of all 16 configurations at optimum spacing and at a typical nozzle pressure ratio of 2.0 and the effects of various modifications to the four basic configurations are shown in figure 7. For the open-end configurations, the 2-diameter deflectors proved superior to the $1\frac{1}{2}$-diameter deflectors of similar shape and the double-circular-arc deflectors proved superior to the single-circular-arc deflectors of similar size.

Although the original design philosophy of the open-end circular-arc deflector called for its retraction up against the lower surface of the wing in a pod-type engine installation in such a way as to permit the free-stream air to pass axially through it, poor reversal (13 to 35 percent) prompted the addition of end plates to prevent escape of the flow 90° to the thrust axis. Increases in reversal from 3 to 45 percentage points were obtained by the addition of end plates. In this particular stage of modification, the $1\frac{1}{2}$-diameter configurations showed superior performance to the 2-diameter configurations of similar shape, and the $1\frac{1}{2}$-diameter single-circular-arc configuration showed superior performance to the $1\frac{1}{2}$-diameter double-circular-arc configuration.

Filleting the sharp internal corners of the deflector to provide a more efficient flow channel resulted in small reversal increases amounting to a maximum of 8 percentage points for the 2-diameter double-circular-arc deflector. The $1\frac{1}{2}$-diameter single-circular-arc, so modified, resulted in the most efficient deflector of the 16 investigated and produced a reversal of about 58 percent.

Because of the apparent additional flow guidance offered by the double-circular-arc deflectors, it had been expected that the double-circular-arc configurations would, in all states of modification, be superior in performance to the single-circular-arc configurations. Since the $1\frac{1}{2}$-diameter double-circular-arc deflector with the ends closed and filleted proved to be 6 percentage points less efficient than the single-circular-arc deflector with the ends closed and filleted, it was supposed that the lack of depth might be the reason for its inferior performance. Accordingly, the sides of the $1\frac{1}{2}$-diameter double-circular-arc deflector with ends closed and filleted were extended to give a depth equal to that of the $1\frac{1}{2}$-diameter single-circular-arc deflector.

Performance of the resulting configuration decreased by 9 percentage points.

In an attempt to gain better performance by a further reduction in deflector size, prompted by the superior performance of the $1\frac{1}{2}$-diameter configuration in the closed and filleted stage of modification, the 1-diameter single-circular-arc deflector with ends closed and filleted was investigated. Only thrust spoilage resulted, amounting to about 97 percent of the forward corrected jet thrust, and no resultant reverse thrust was obtained.

The relative performance of the 2.2-diameter cup deflector is also shown in figure 7. A 38-percent reversal was obtained, but changes in size might very well improve the efficiency of this configuration.

Because the inner surfaces of the single-circular-arc deflectors, with ends closed and filleted, were approaching hemispherical surfaces, and since a hemispherical deflector would readily lend itself to retraction around the exhaust nozzle, as will be shown later, a 1.5-diameter hemispherical deflector was tested. Its reversal performance, which at a nozzle pressure ratio of 2 amounted to 39 percent, is shown in figure 7.

From the foregoing results, it appears that deflector size and geometry are interrelated and that their effects cannot be independently predicted. An optimum size was shown to exist, however, for a particular geometry (the single-circular-arc closed and filleted end deflector).

Because the main purpose of the 16 configurations just discussed was to rapidly screen various deflector sizes, geometries, and modifications of geometries, no pressure or flow surveys were made for this part of the investigation.

Application of Target-Type Reversal Device to Typical Nacelle-Mounted Turbojet Engine Installation and Analysis of Performance

To determine the performance of a deflector mounted on a typical engine installation, with reverse flow around the retraction fairing, a model tail pipe, cowl, and deflector installation was constructed (fig. 2).

A 1.5-diameter hemispherical deflector was selected for the model installation because of its moderately good reversal characteristics and especially because of the ease with which it could be retracted and faired. The proposed method of retraction is shown in figure 8. In the retracted position, the deflector, composed of a large spherical sector A and a small spherical sector B, would provide a smooth contour for the rear of the installation. For extension to the reversed-thrust position, the deflector would be translated aft and sectors A and B would be rotated toward each other, one sliding over the other, until the nozzle-exit hole in sector A was covered and a hemisphere formed.

Performance of the complete installation was similar to the performance of the 1.5-diameter hemisphere mounted behind the simple exhaust nozzle which has previously been shown in figure 4(p). A velocity survey, presented in figure 9(a), showed that the reversed jet flowing from the hemisphere was turned through an angle of only 120° and emerged in a sharply defined surface which was completely isolated from the cowling, thus accounting for the similar performance of the hemispherical deflector on both the simple exhaust nozzle and the model tailpipe and cowling assembly. The direction and shape of the reversed jet also indicated that the jet did not follow the contour of the hemisphere but was merely deflected by a stagnant region within the hemisphere.

It is interesting to note that if no pressure loss occurred in turning, a 120° turn would produce 50-percent reversal. Because only 39-percent reversal was obtained at the pressure ratio at which the velocity survey was taken, 11 percent of the available thrust was lost through reduction in air flow, shock, and friction.

Because such a wide-angle discharge appeared to be undesirable for some applications, a double-skin hemisphere with a perforated inner skin (fig. 3(j), configuration Q) was designed. It was expected that the stagnant air would bleed between the two skins, thus allowing the main jet to follow more closely the contour of the inner skin and be turned closer to 180°. The design accomplished its purpose by curving the reversed jet rather than appreciably changing the immediate discharge angle as can be seen from figure 9(b), which is the result of velocity surveys taken at several locations along the cowl. Pressure under the retraction fairing remained atmospheric.

Because some throttling loss through the holes in the inner skin probably occurred and because the immediate discharge angle of the jet was probably somewhat increased, performance of the 1.5-diameter double-skin hemisphere was approximately the same as that of the single-skin hemisphere and is shown in figure 10. It appears, therefore, that by adjustment of inner-skin hole area and the discharge area between the inner and outer skins, the reversed jet along the cowl could be made to flow at any desired angle without any severe thrust-reversal penalties.

CONCLUDING REMARKS

Of the 17 target-type thrust-reversal devices investigated, the $1\frac{1}{2}$-nozzle-diameter single-circular-arc deflector with closed and filleted ends produced maximum reversal, amounting to approximately 58 percent of the forward jet thrust.

The effect of closing the ends of various open-end circular-arc deflectors, which caused increases in thrust reversal from 3 to 45 percentage points, was dependent upon deflector size and configuration.

The effect of filleting the internal angles of various closed-end circular-arc deflectors was small, resulting in a maximum reversal increase of 8 percentage points and was also dependent upon deflector size and configuration.

Maximum or near-maximum reversal for any configuration could be obtained with the deflector positioned such that the corrected air flow of the nozzle deflector installation remained the same as the corrected air flow of the nozzle alone, demonstrating that these deflectors can be efficiently used without affecting engine operation.

Deflector spacing (distance from exhaust-nozzle exit to rear face of deflector) required for an air-flow ratio of 100 percent varied from about 0.66 to 1.3 nozzle diameters and appeared mechanically feasible.

Maximum variation in reversal over a range of nozzle pressure ratios from 1.7 to 3.0 for a given deflector at optimum spacing was about 10 percent. The variation was considerably less, however, for the closed-end deflectors (with the exception of the 1.5-diameter hemisphere) and amounted to about 5 percent.

A 1.5-diameter hemispherical deflector, chosen as a practical reversal device and installed on a model of a typical nacelle-type engine installation, produced 39 percent reversal at a nozzle pressure ratio of 2.0 by turning the jet 120°. Of the available thrust, 50 percent was therefore lost through insufficient turning and 11 percent through air-flow reduction, shock, and friction. A 1.5-diameter double-skin hemisphere produced a reversal of 40 percent at the same pressure ratio, but caused the reversed jet to flow in a curved path resulting in a turn of about 180°.

Lewis Flight Propulsion Laboratory
National Advisory Committee for Aeronautics
Cleveland, Ohio, December 21, 1953

Page intentionally left blank

APPENDIX - SYMBOLS

The following symbols are used in this report:

D exhaust-nozzle diameter

d deflector exit diameter, exhaust-nozzle diameters

h deflector exit height, exhaust-nozzle diameters

l deflector spacing in nozzle diameters, measured from exhaust nozzle exit to rear inner face of deflector

P_n total pressure immediately upstream of the exhaust nozzle

p_0 ambient pressure in the test cell

T total temperature upstream of the exhaust nozzle

W_a air flow

w deflector exit width, exhaust-nozzle diameters

δ ratio of total pressure at nozzle inlet to absolute pressure at NACA standard sea-level conditions

θ ratio of total temperature at nozzle inlet to absolute temperature at NACA standard sea-level conditions

REFERENCES

1. Iserland, K.: Braking the Landing Run of Jet Aircraft by Thrust Deviation. Interavia, vol. VIII, no. 3, 1953, pp. 151-154.

2. Polak, I. P.: Developement of Turbo-Jet Engine Thrust Destroying and Reversing Nozzle No. AEL 102. AEL-1108, Aero. Eng. Lab., Naval Air Material Center, Naval Air Station (Phila.), Jan. 13, 1950. (Proj. TED No. NAM-PP-375 and TED No. NAM-04614.)

TABLE I. - DEFLECTOR CONFIGURATIONS

Configuration	Deflector exit width and height, or diameter, exhaust-nozzle diameters	Geometry	Modifications
A	$1\frac{1}{2}$	Single circular arc	Ends open
B	2	Single circular arc	Ends open
C	$1\frac{1}{2}$	Double circular arc	Ends open
D	2	Double circular arc	Ends open
E	$1\frac{1}{2}$	Single circular arc	Ends closed
F	2	Single circular arc	Ends closed
G	$1\frac{1}{2}$	Double circular arc	Ends closed
H	2	Double circular arc	Ends closed
I	$1\frac{1}{2}$	Single circular arc	Ends closed and filleted
J	2	Single circular arc	Ends closed and filleted
K	$1\frac{1}{2}$	Double circular arc	Ends closed and filleted
L	2	Double circular arc	Ends closed and filleted
M	$1\frac{1}{2}$	Double circular arc	Ends closed and filleted and sides extended
N	1	Single circular arc	Ends closed and filleted
O	2.2	Cup	
P	1.5	Hemisphere	
Q	1.5	Double-skin hemisphere	

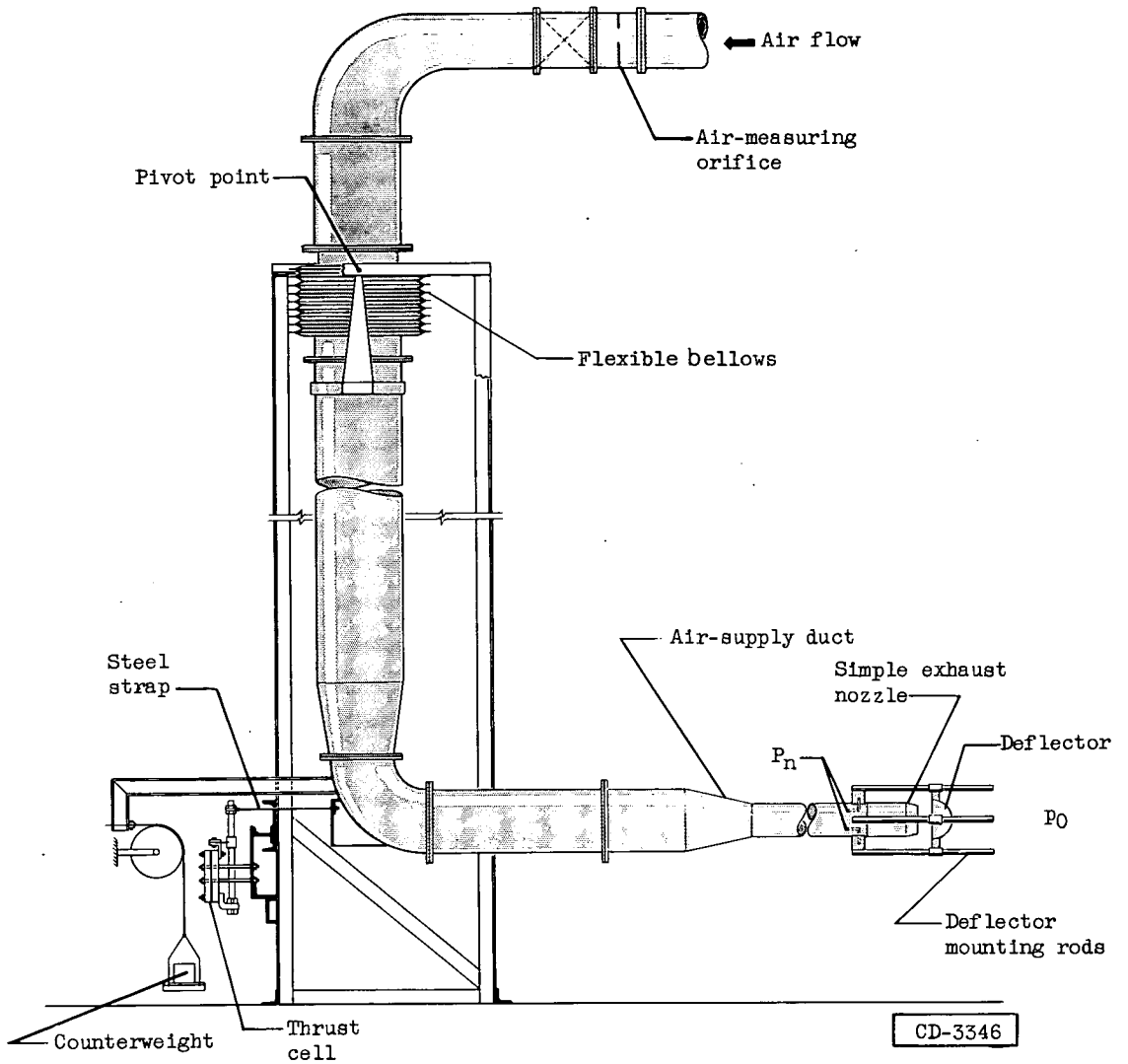

Figure 1. - Schematic diagram of setup for thrust-reversal investigation.

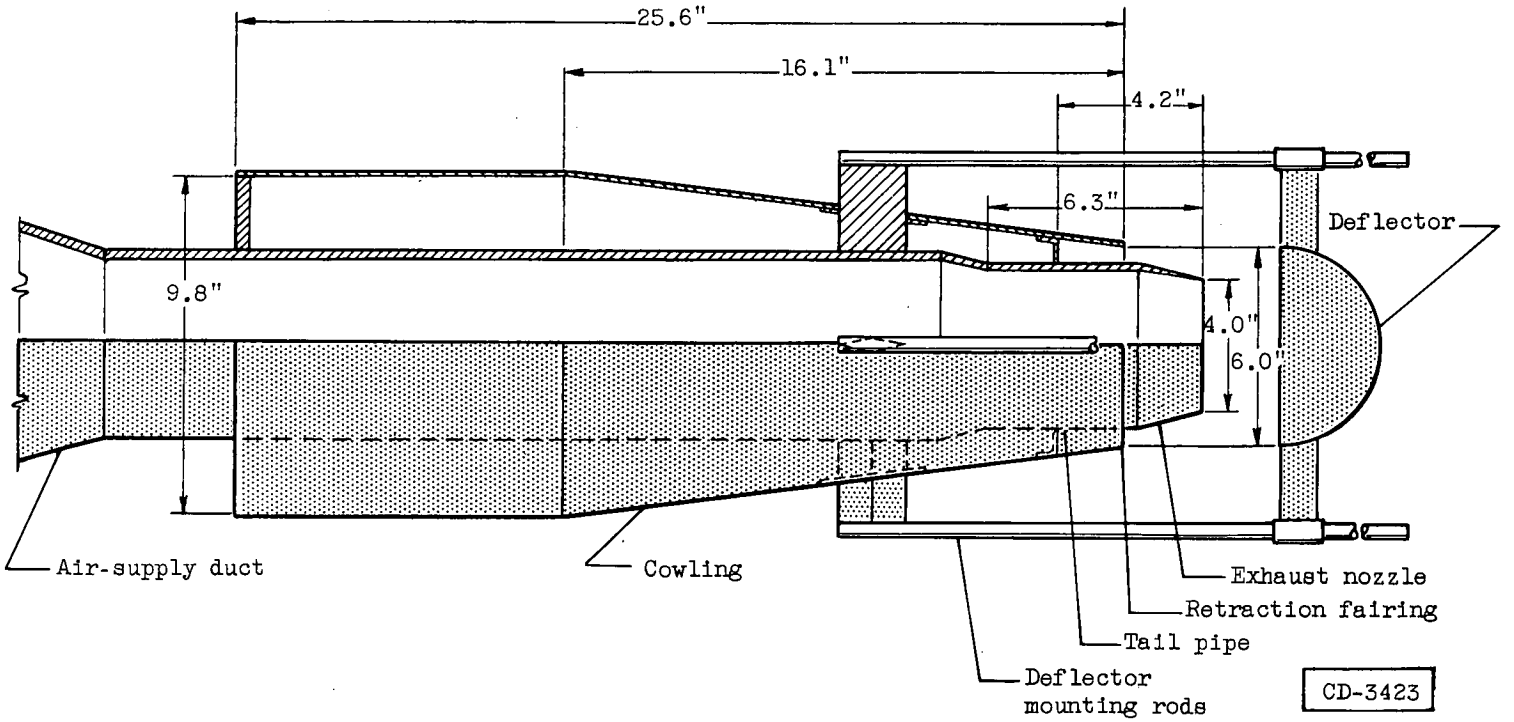

Figure 2. - Model engine tail-pipe and cowling assembly with single-skin hemispherical deflector attached.

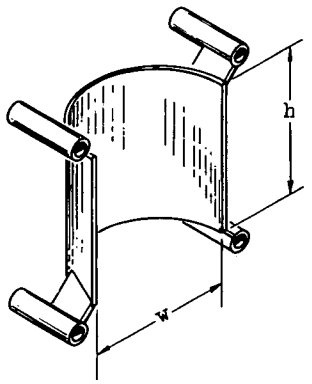

(a) Configurations A and B, single circular arc, ends open.

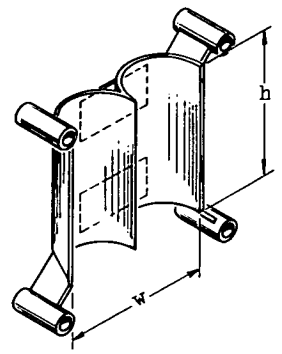

(b) Configurations C and D, double circular arc, ends open.

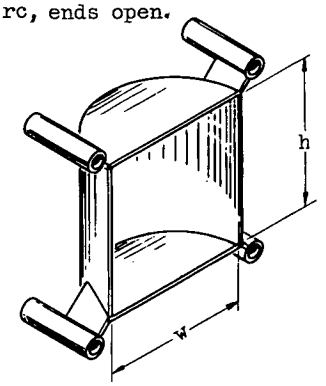

(c) Configurations E and F, single circular arc, ends closed.

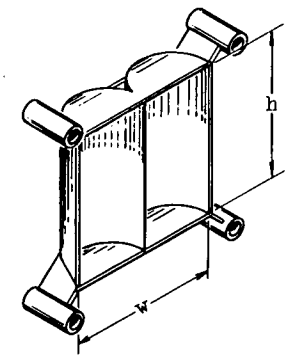

(d) Configurations G and H, double circular arc, ends closed.

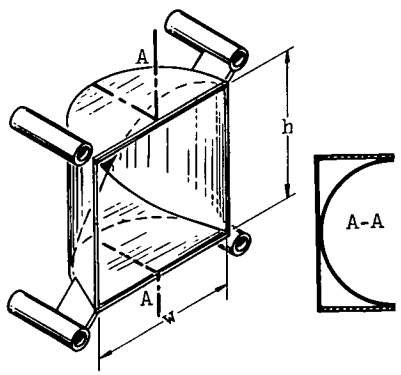

(e) Configurations I, J, and N, single circular arc, ends closed and filleted.

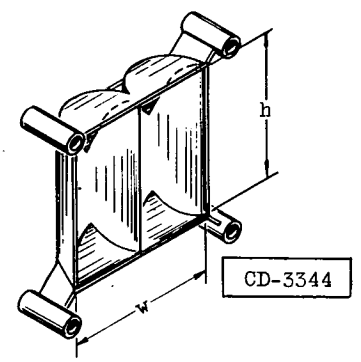

(f) Configurations K and L, double cricular arc, ends closed and filleted.

Figure 3. - Typical jet deflector geometries.

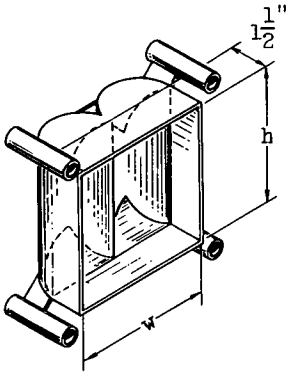

(g) Configuration M, double circular arc, ends closed and filleted and sides extended.

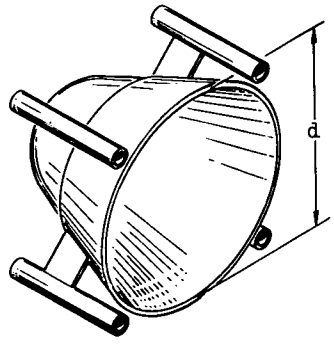

(h) Configuration O, cup.

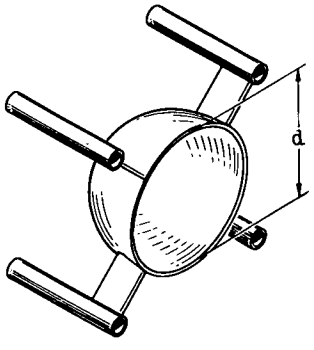

(i) Configuration P, hemisphere.

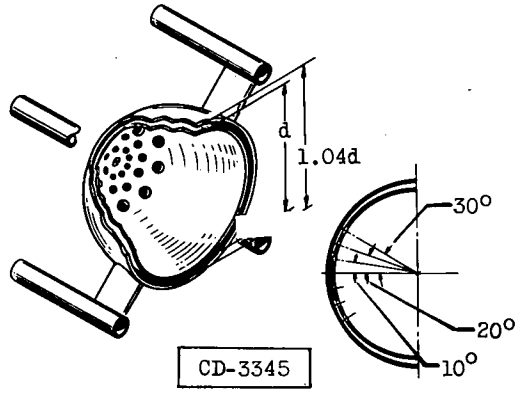

(j) Configuration Q, double-skin hemisphere.

Figure 3. - Concluded. Typical jet deflector geometries.

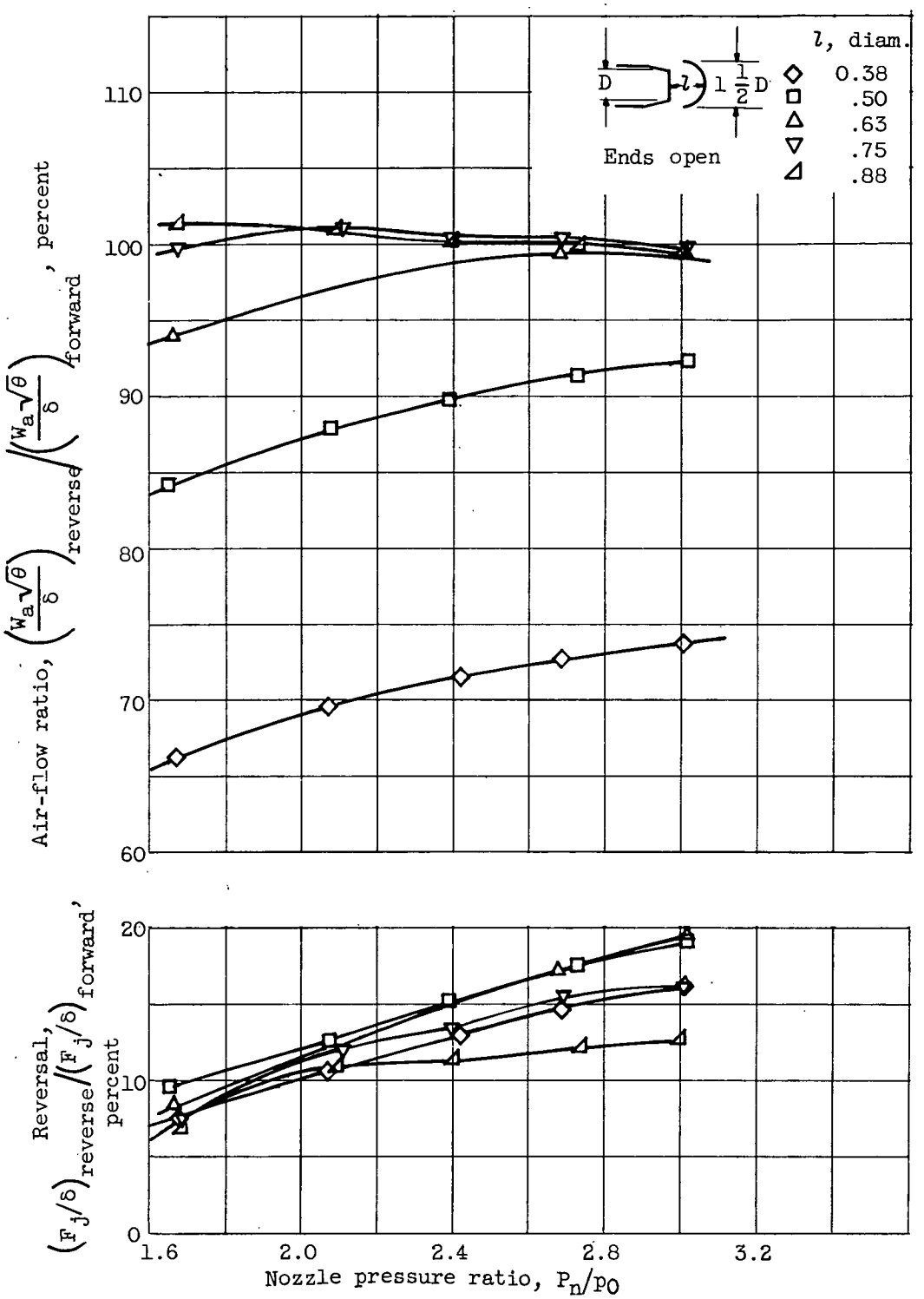

(a) Configuration A.

Figure 4. - Air-flow and thrust-reversal characteristics of deflectors over range of exhaust-nozzle pressure ratios.

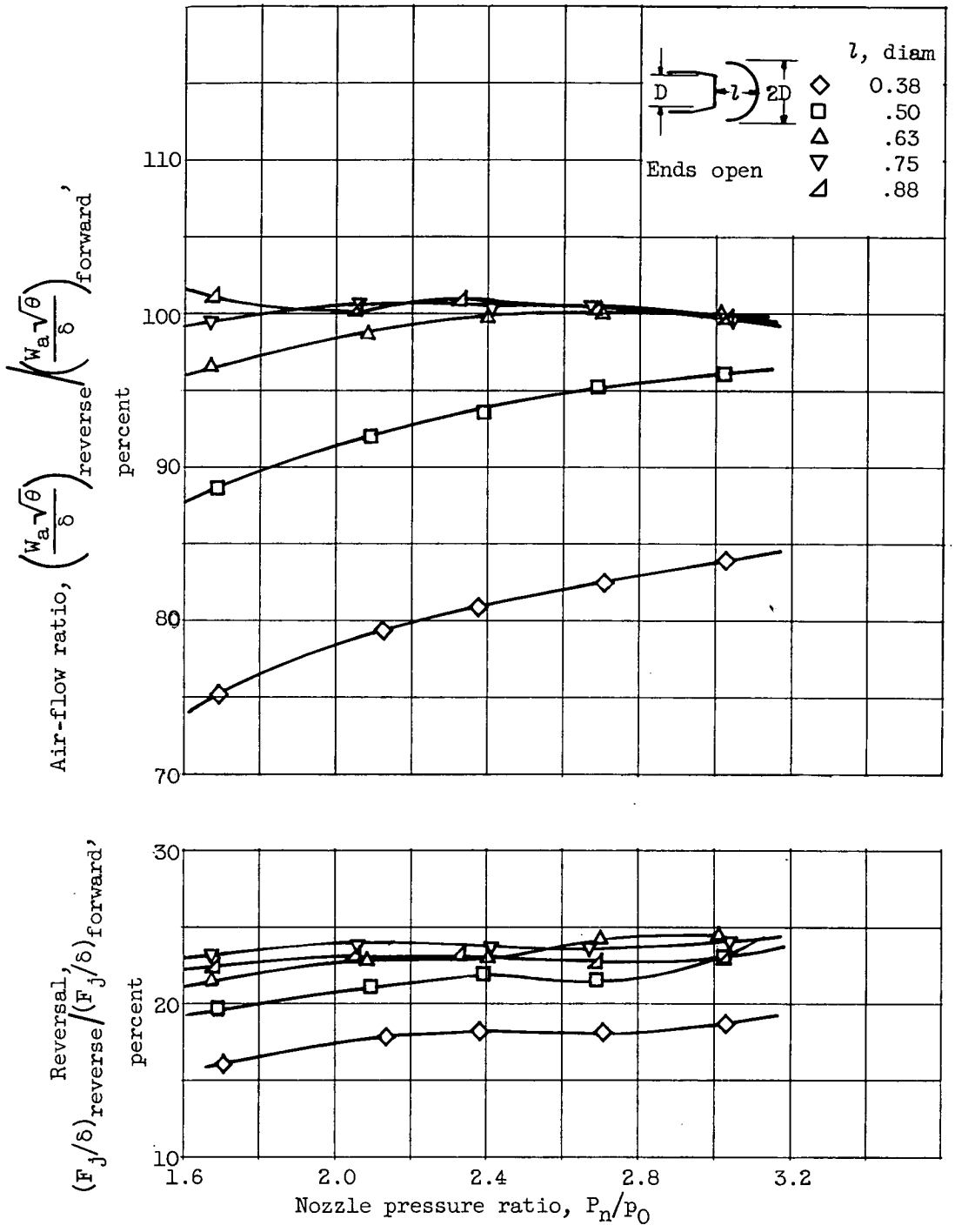

(b) Configuration B.

Figure 4. - Continued. Air-flow and thrust-reversal characteristics of deflectors over range of exhaust-nozzle pressure ratios.

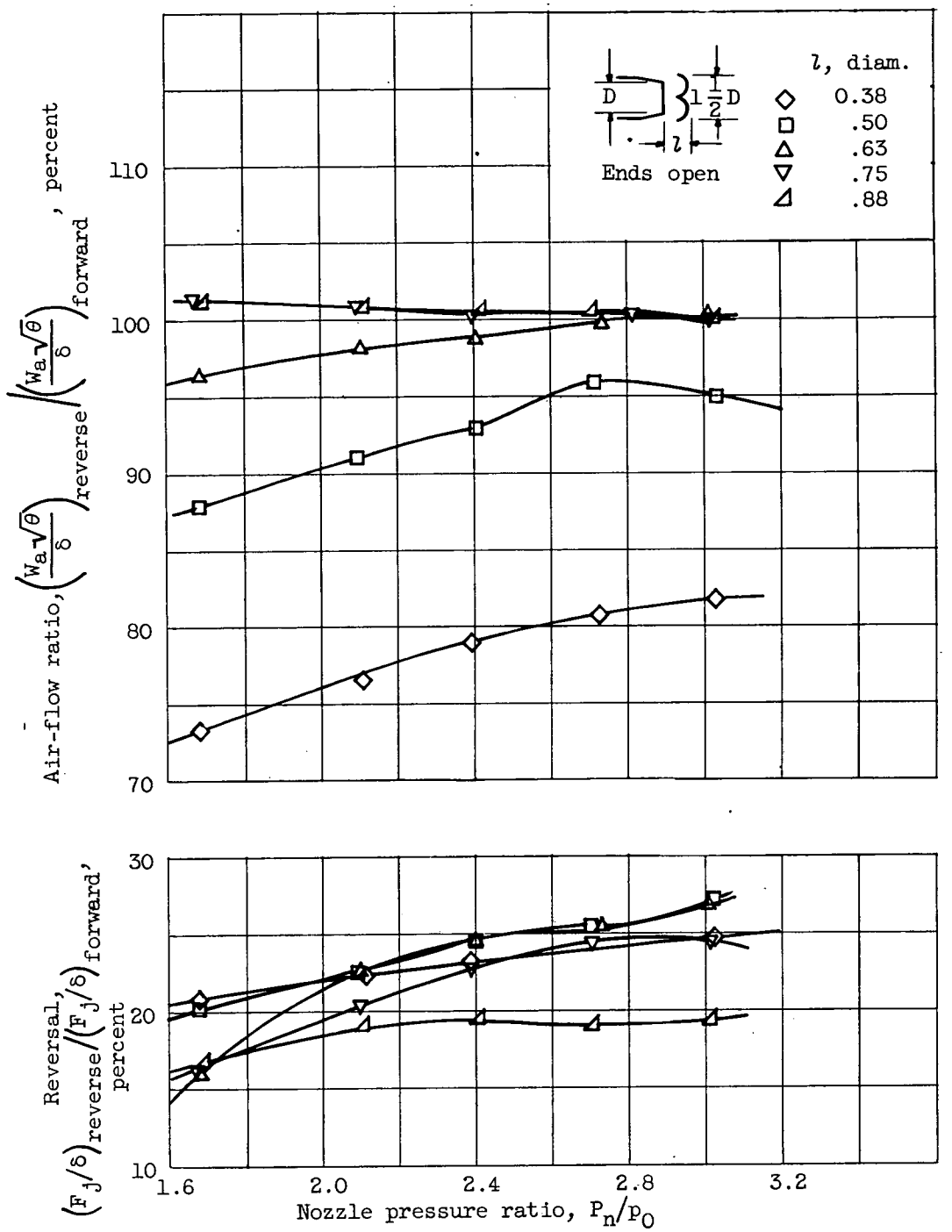

(c) Configuration C.

Figure 4. - Continued. Air-flow and thrust-reversal characteristics of deflectors over range of exhaust-nozzle pressure ratios.

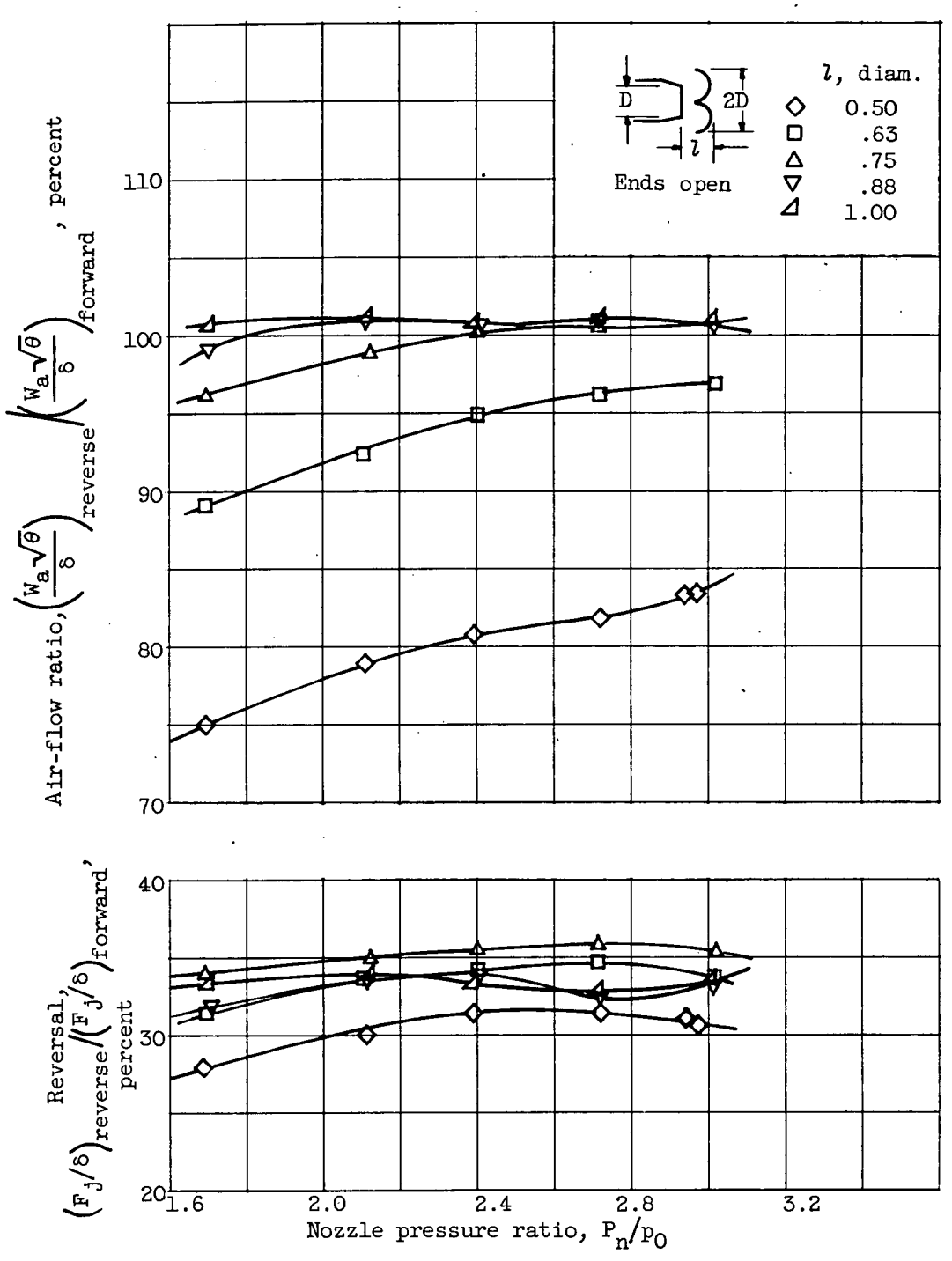

(d) Configuration D.

Figure 4. - Continued. Air-flow and thrust-reversal characteristics of deflectors over range of exhaust-nozzle pressure ratios.

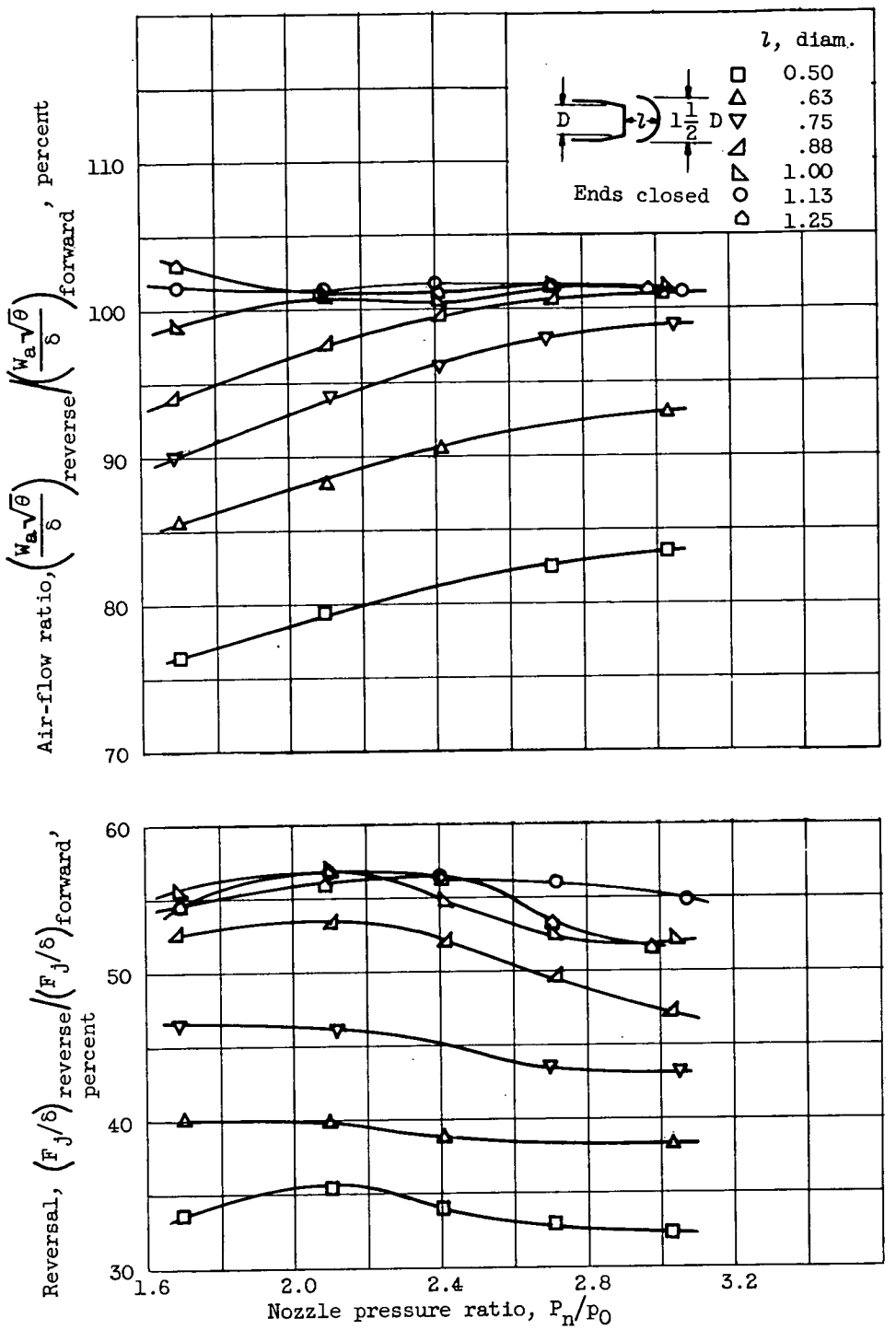

(e) Configuration E.

Figure 4. - Continued. Air-flow and thrust-reversal characteristics of deflectors over range of exhaust-nozzle pressure ratios.

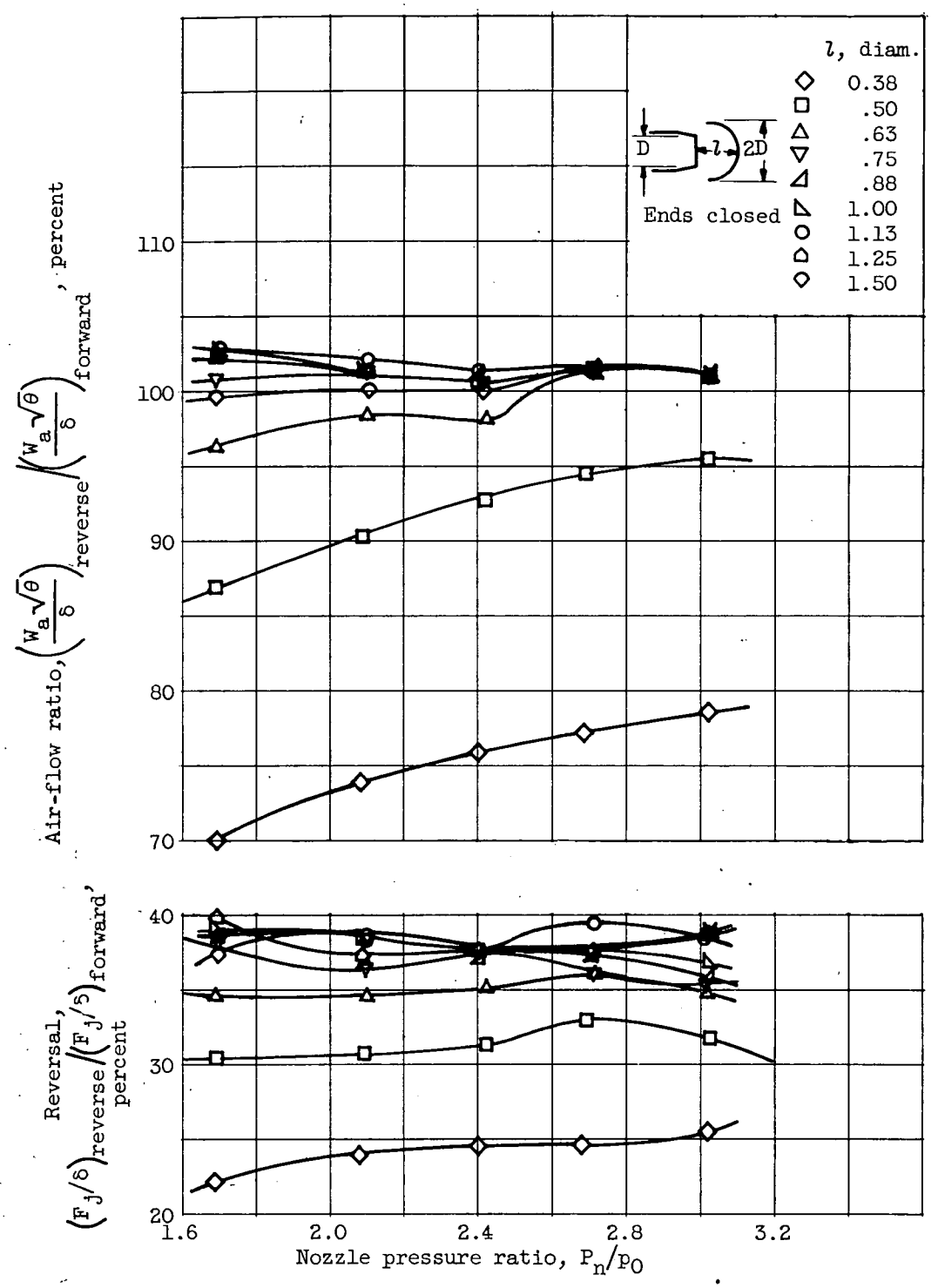

(f) Configuration F.

Figure 4. - Continued. Air-flow and thrust-reversal characteristics of deflectors over range of exhaust-nozzle pressure ratios.

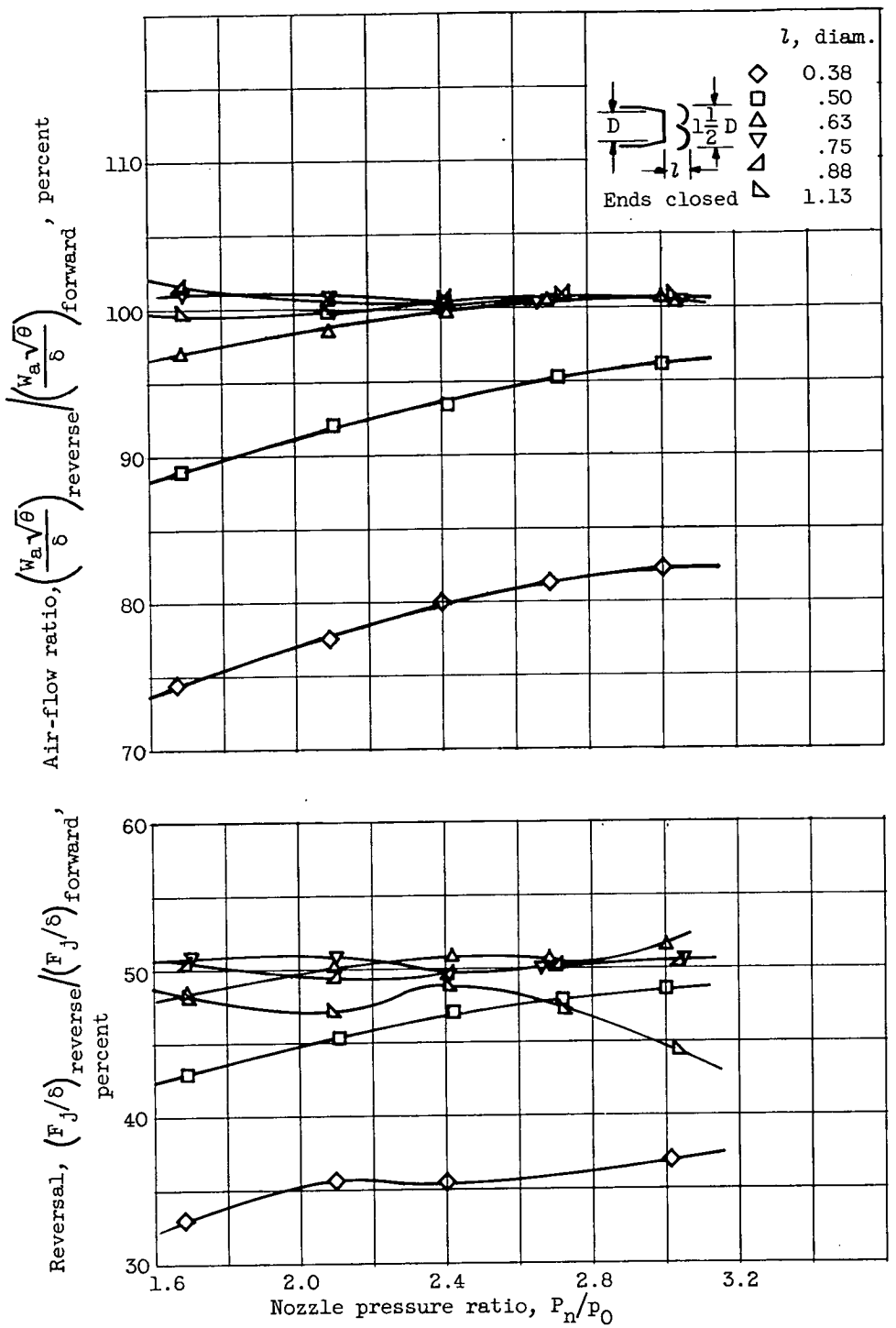

(g) Configuration G.

Figure 4. - Continued. Air-flow and thrust-reversal characteristics of deflectors over range of exhaust-nozzle pressure ratios.

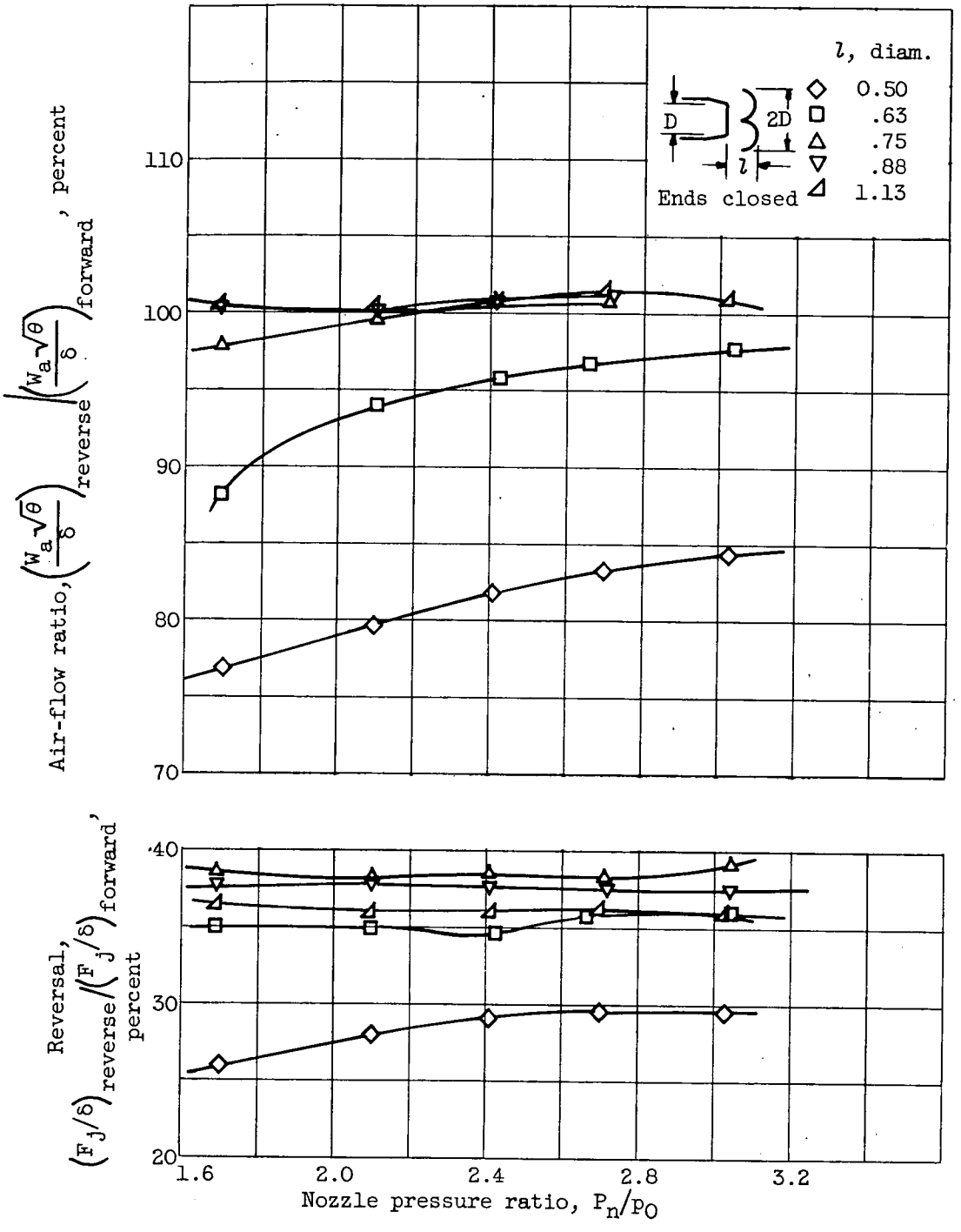

(h) Configuration H.

Figure 4. - Continued. Air-flow and thrust-reversal characteristics of deflectors over range of exhaust-nozzle pressure ratios.

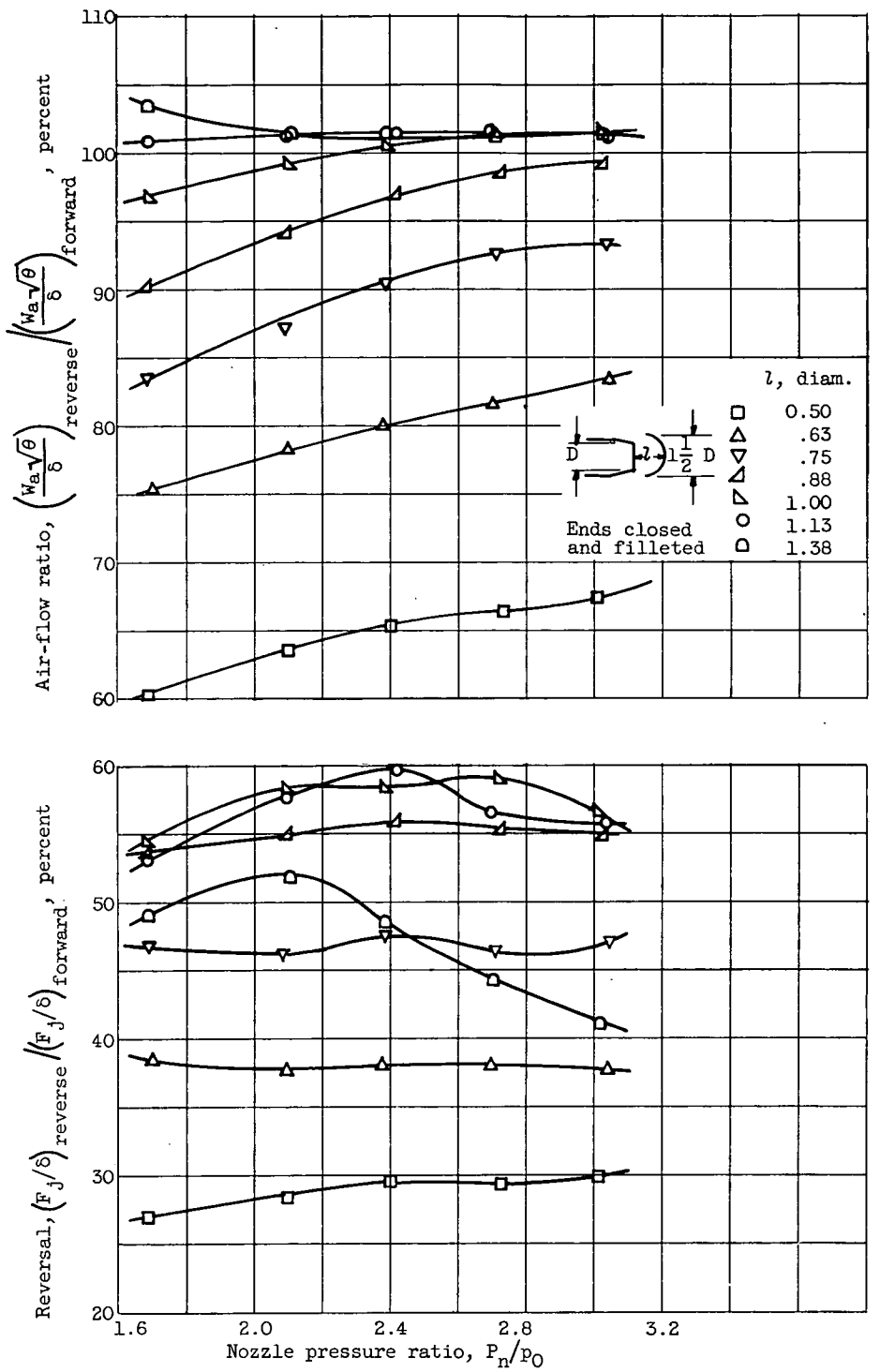

(i) Configuration I.

Figure 4. - Continued. Air-flow and thrust-reversal characteristics of deflectors over range of exhaust-nozzle pressure ratios.

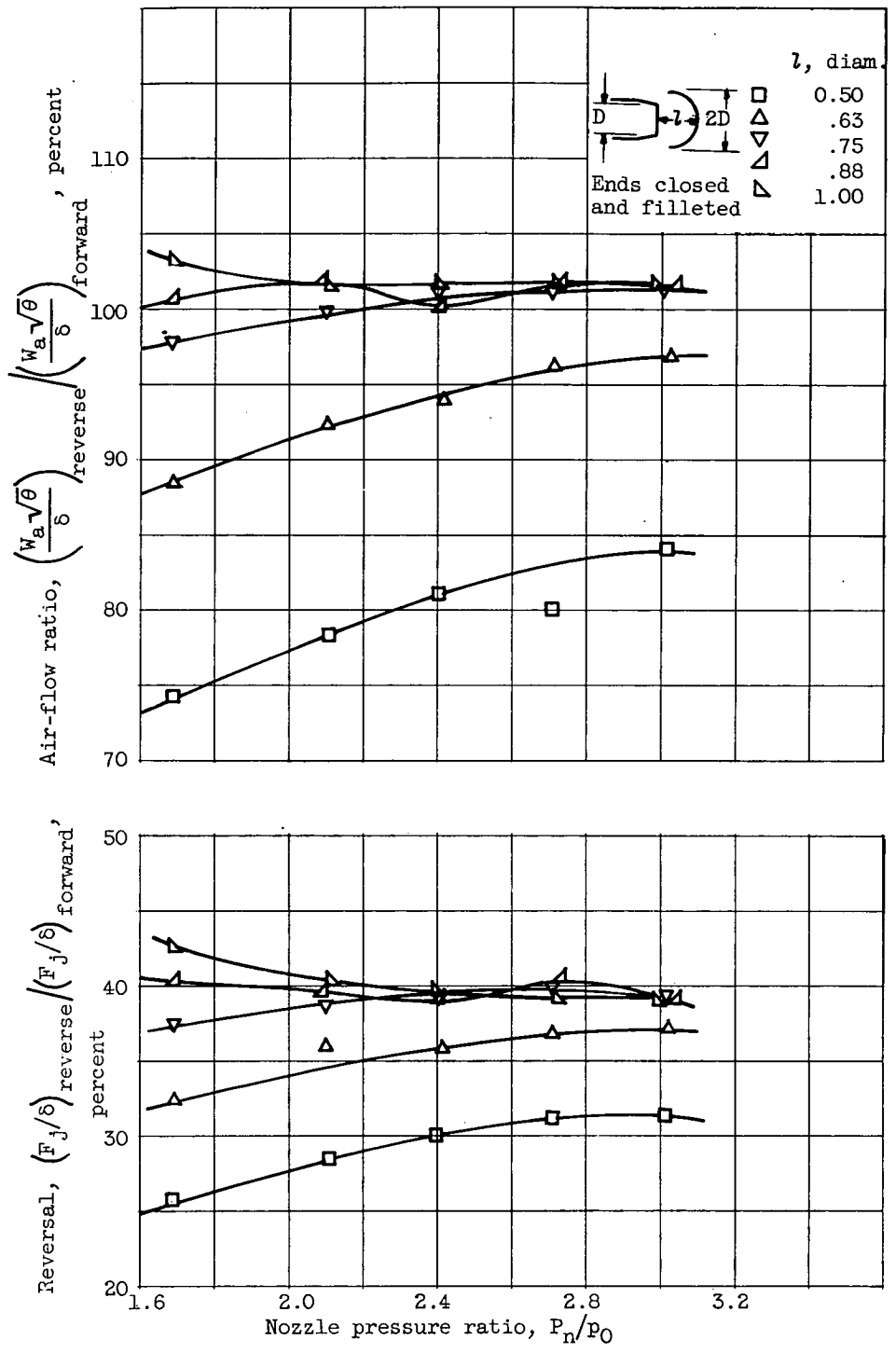

(j) Configuration J.

Figure 4. - Continued. Air-flow and thrust-reversal characteristics of deflectors over range of exhaust-nozzle pressure ratios.

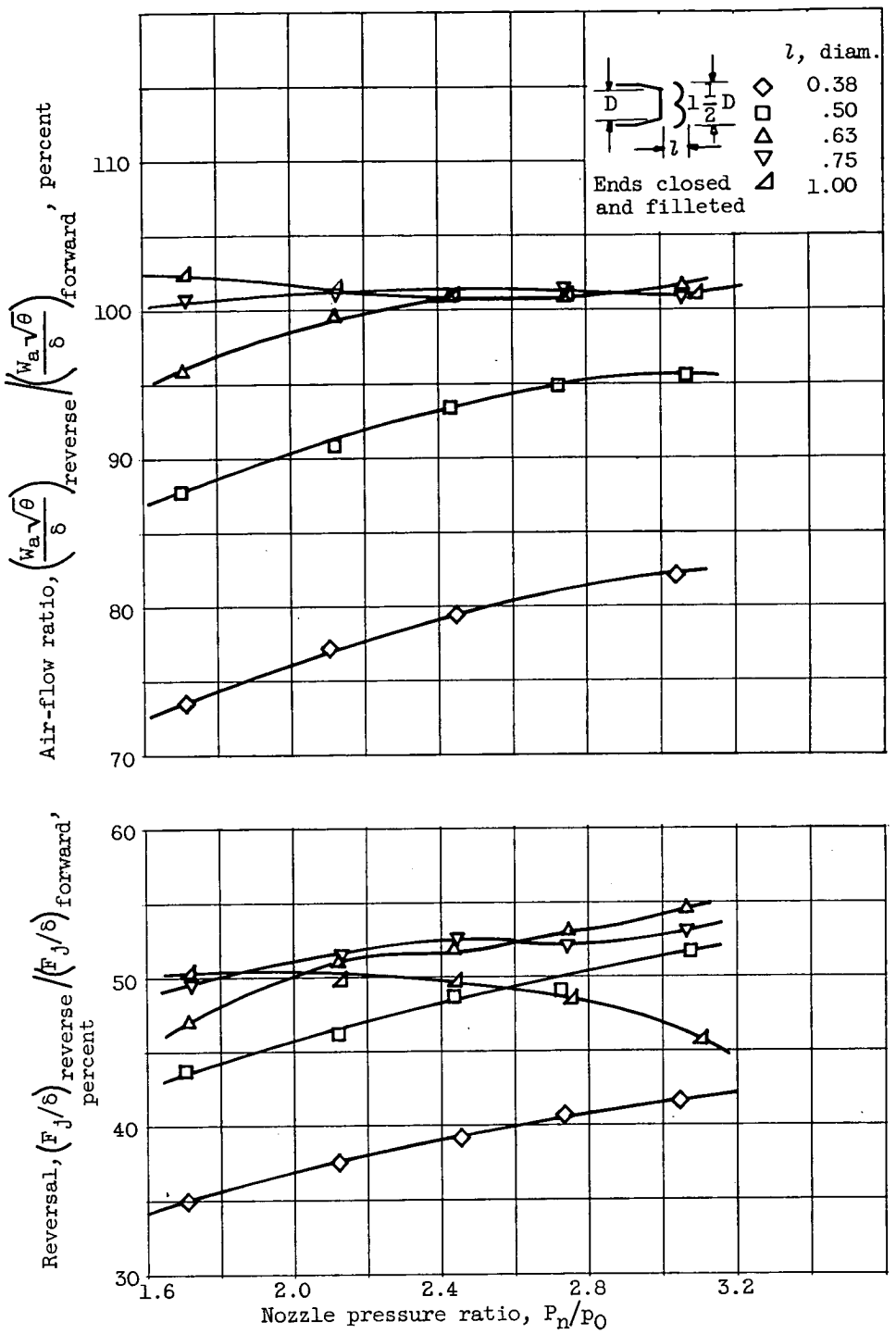

(k) Configuration K.

Figure 4. - Continued. Air-flow and thrust-reversal characteristics of deflectors over range of exhaust-nozzle pressure ratios.

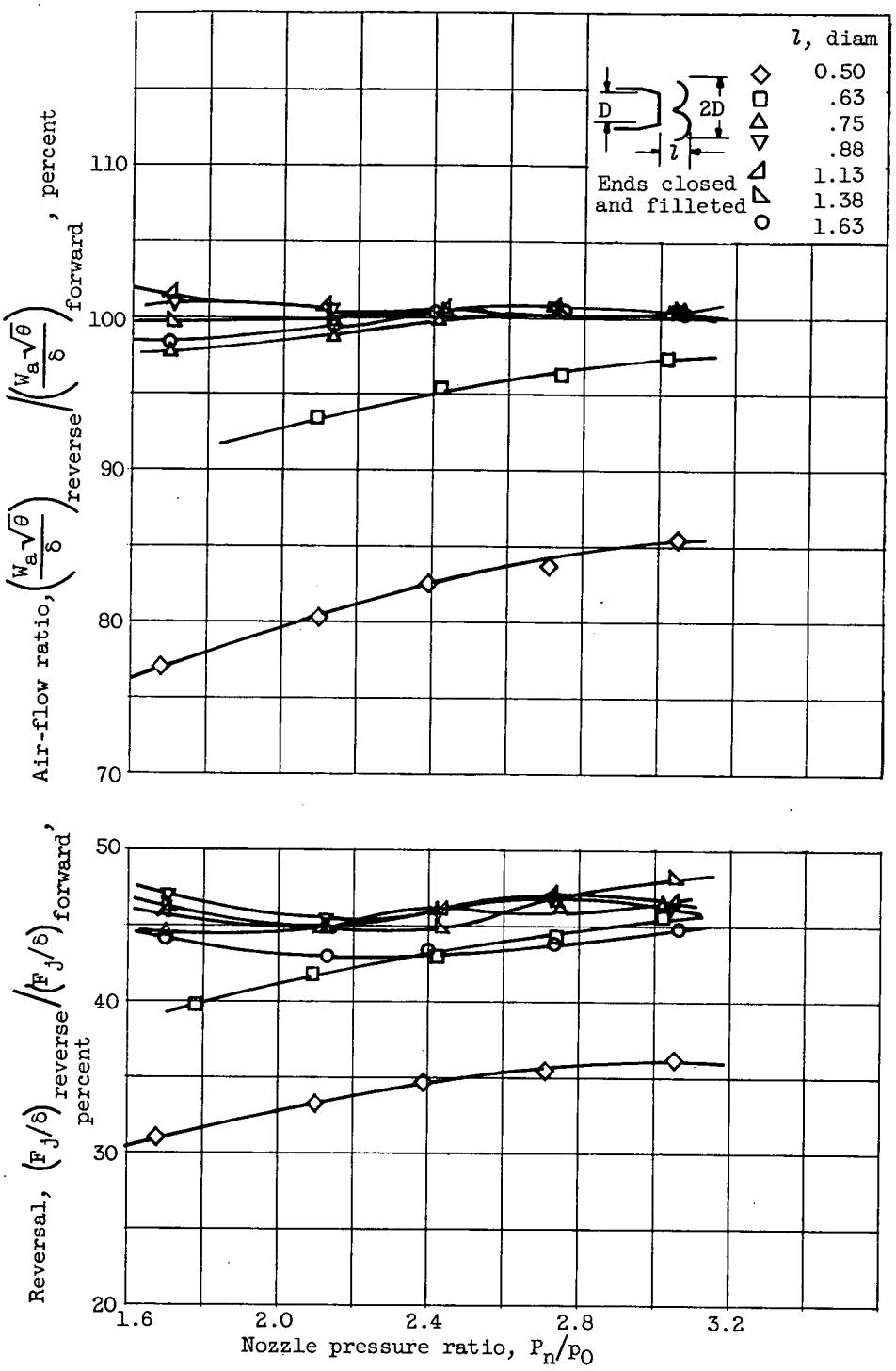

(l) Configuration L.

Figure 4. - Continued. Air-flow and thrust-reversal characteristics of deflectors over range of exhaust-nozzle pressure ratios.

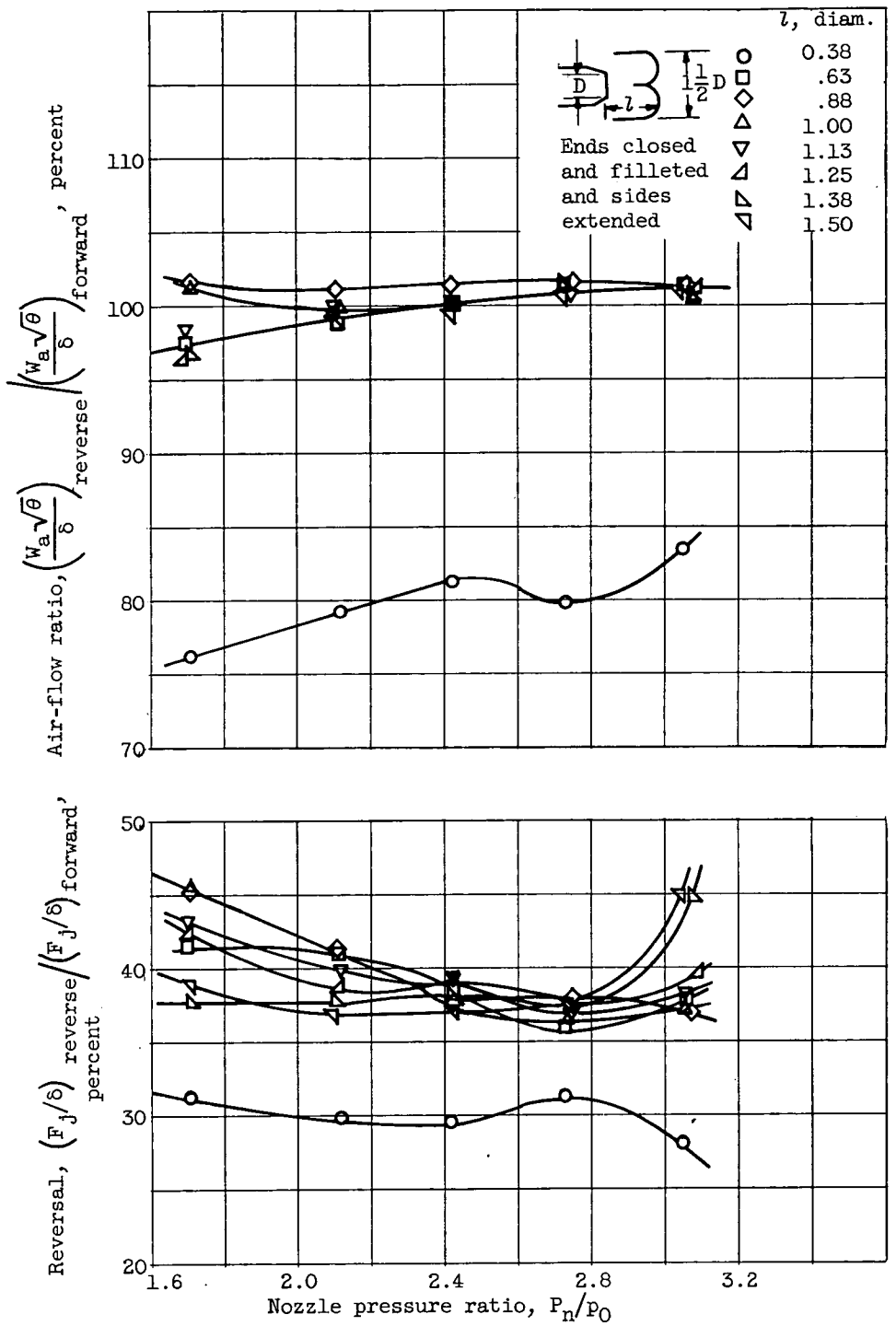

(m) Configuration M.

Figure 4. - Continued. Air-flow and thrust-reversal characteristics of deflectors over range of exhaust-nozzle pressure ratios.

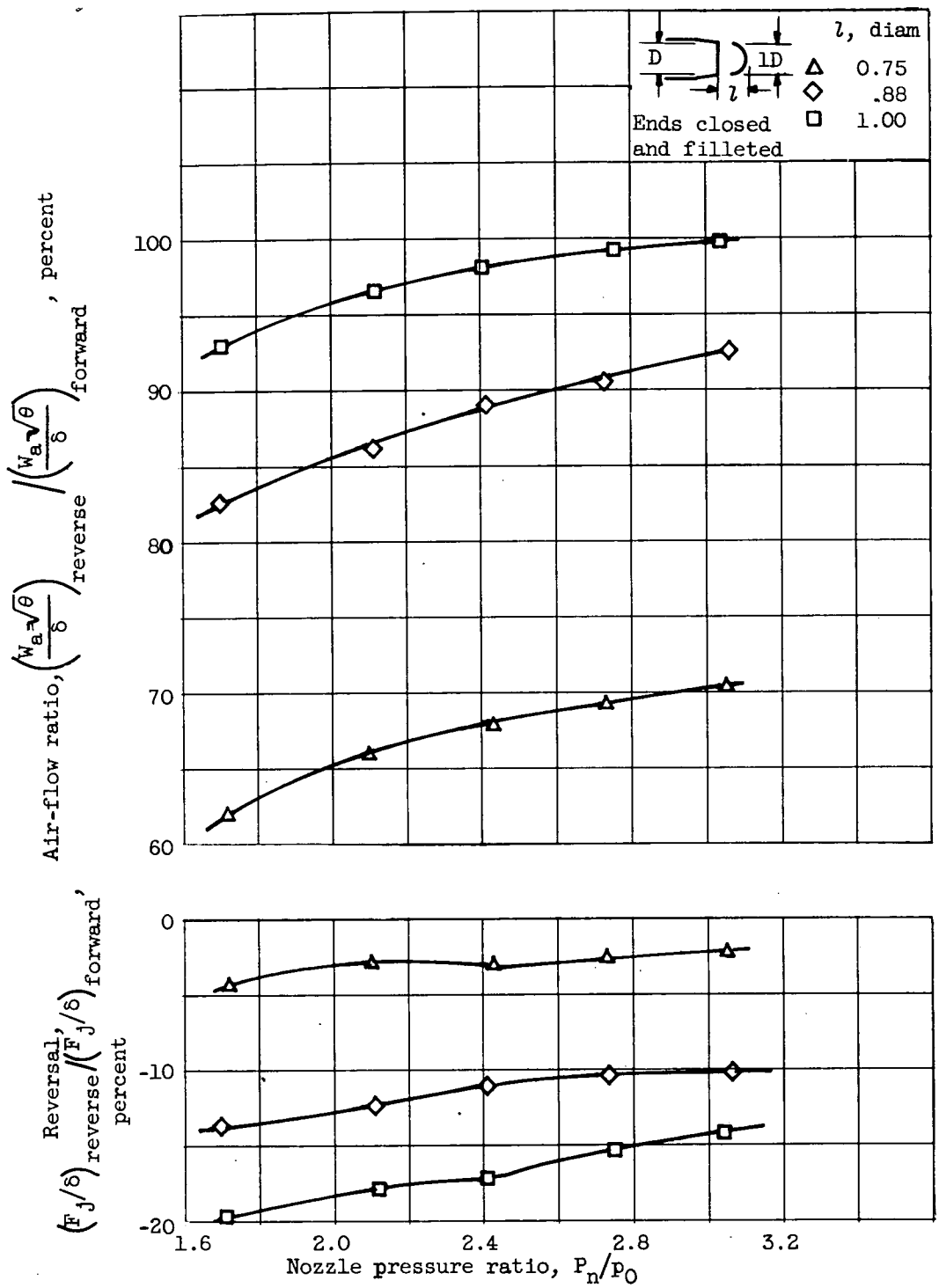

(n) Configuration N.

Figure 4. - Continued. Air-flow and thrust-reversal characteristics of deflectors over range of exhaust-nozzle pressure ratios.

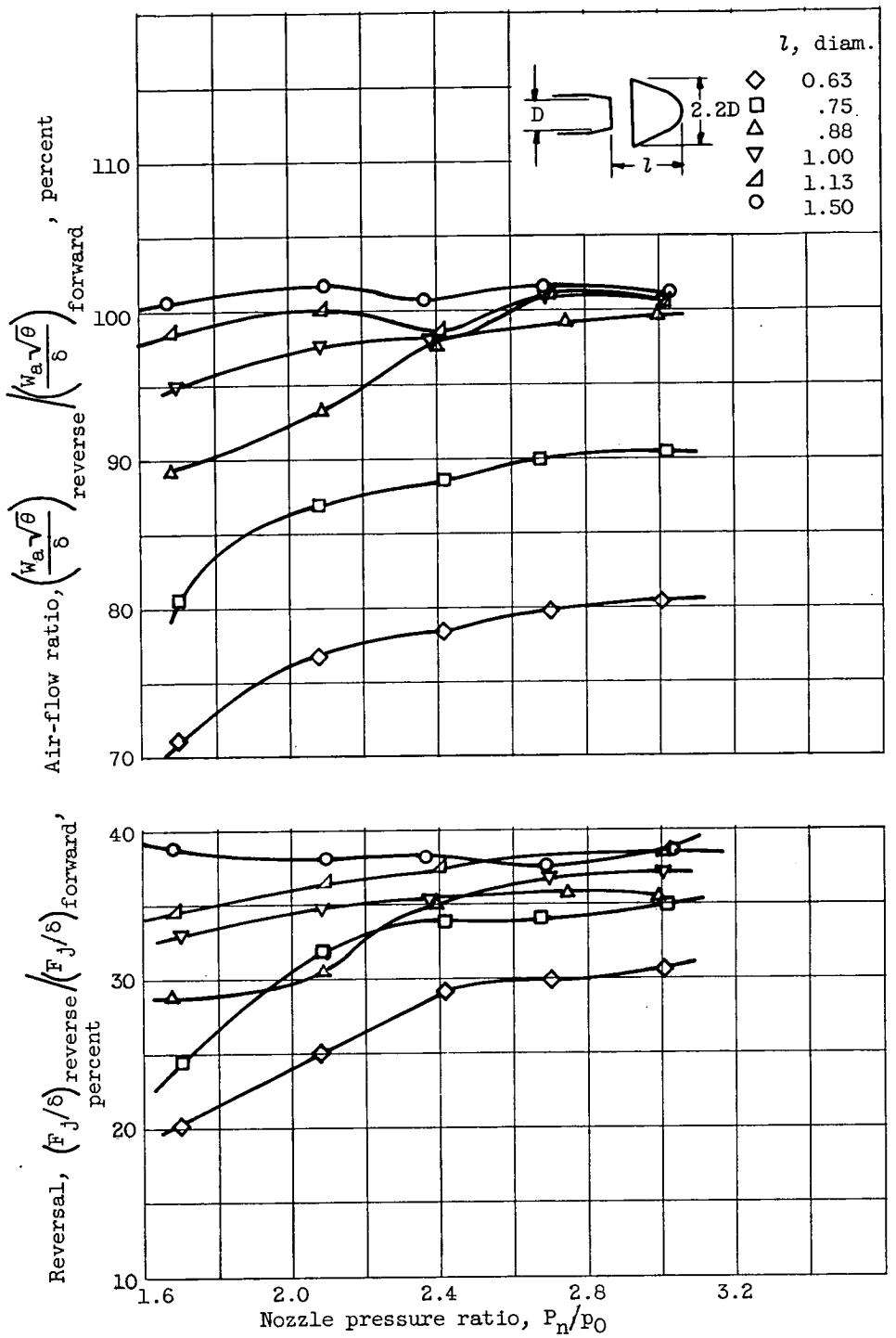

(o) Configuration O.

Figure 4. - Continued. Air-flow and thrust-reversal characteristics of deflectors over range of exhaust-nozzle pressure ratios.

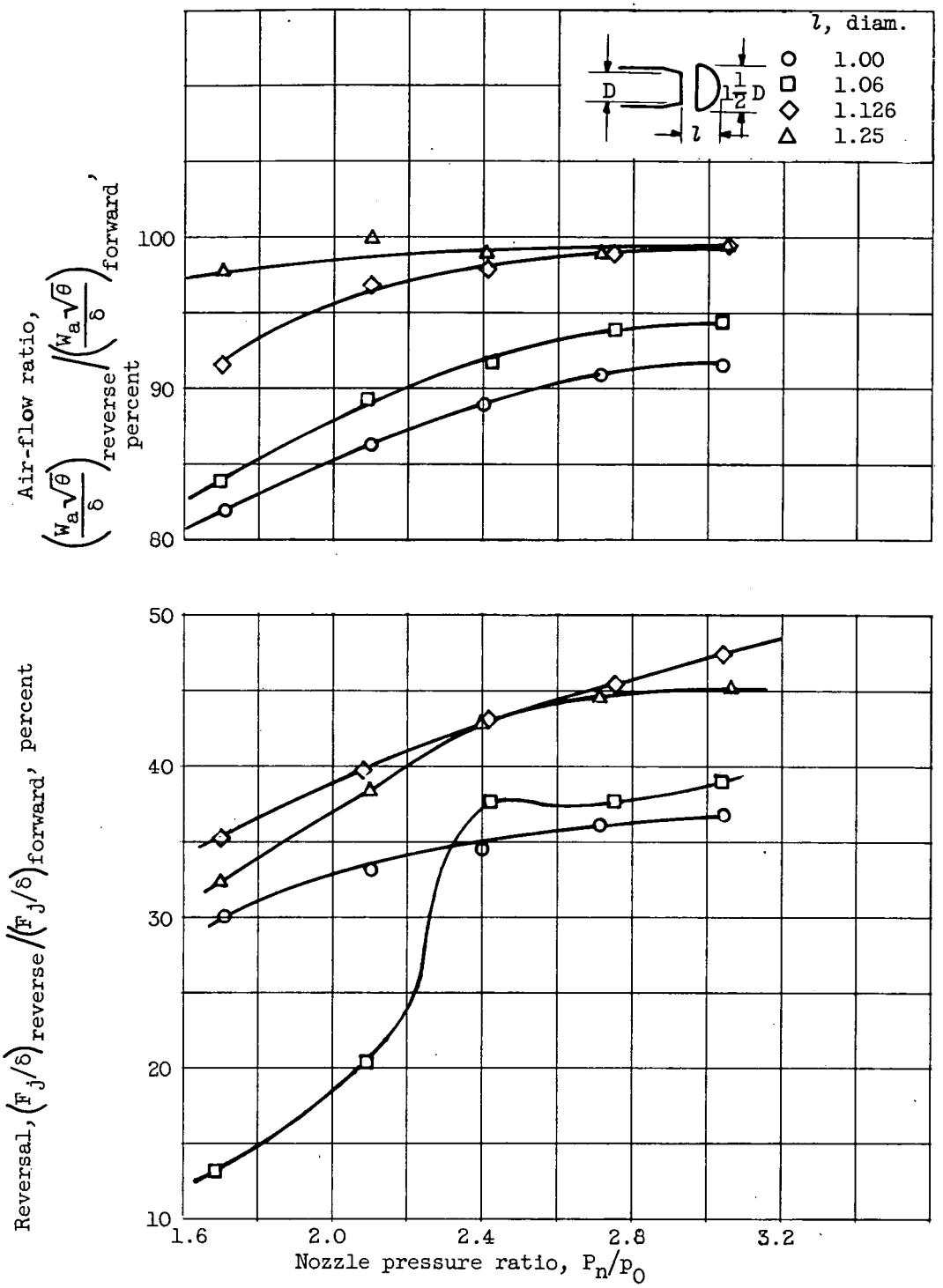

(p) Configuration P.

Figure 4. - Concluded. Air-flow and thrust-reversal characteristics of deflectors over range of exhaust-nozzle pressure ratios.

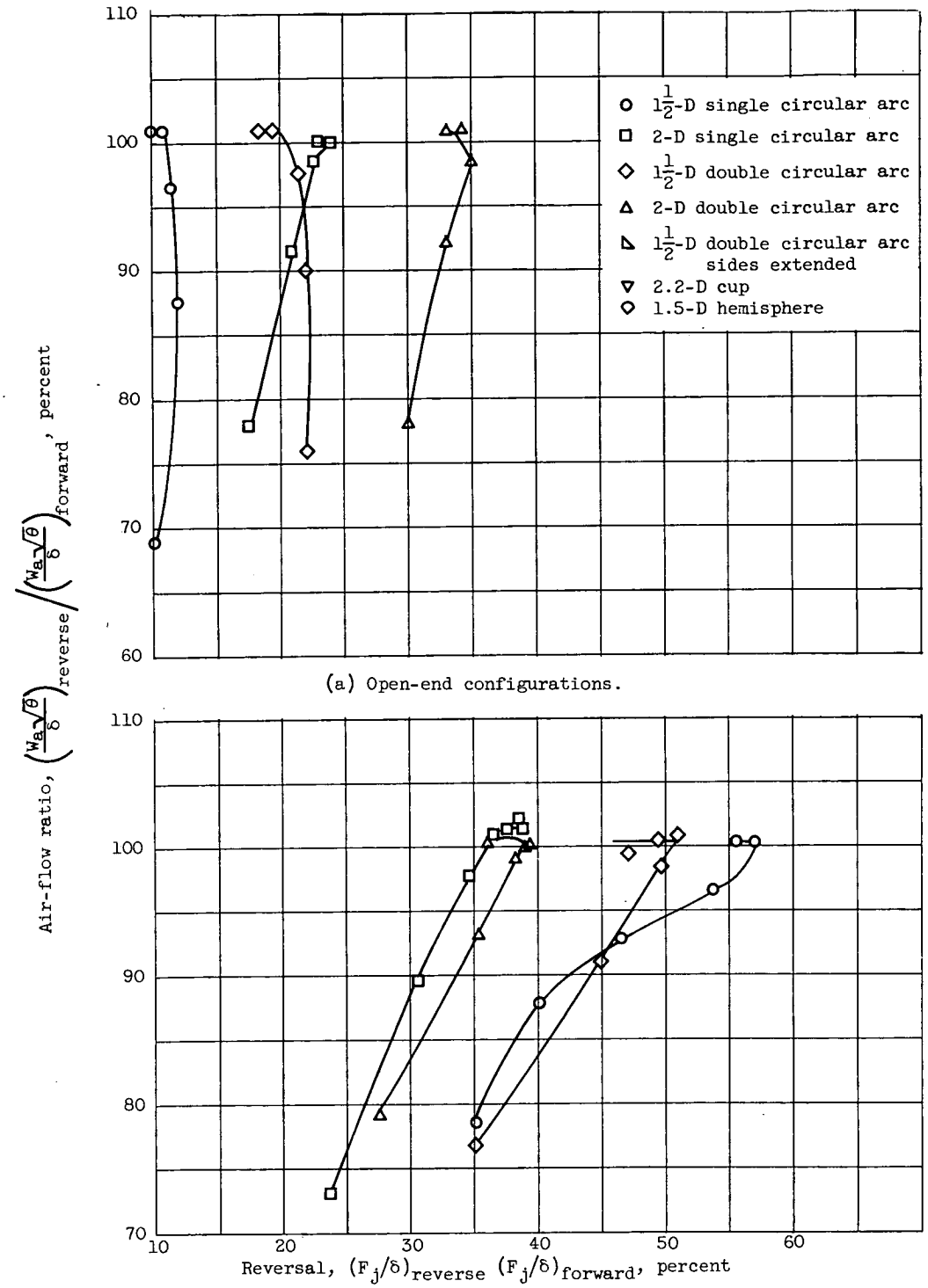

Figure 5. - Variation of corrected air flow with thrust reversal for various deflectors. Exhaust-nozzle pressure ratio, P_n/p_0, 2.0.

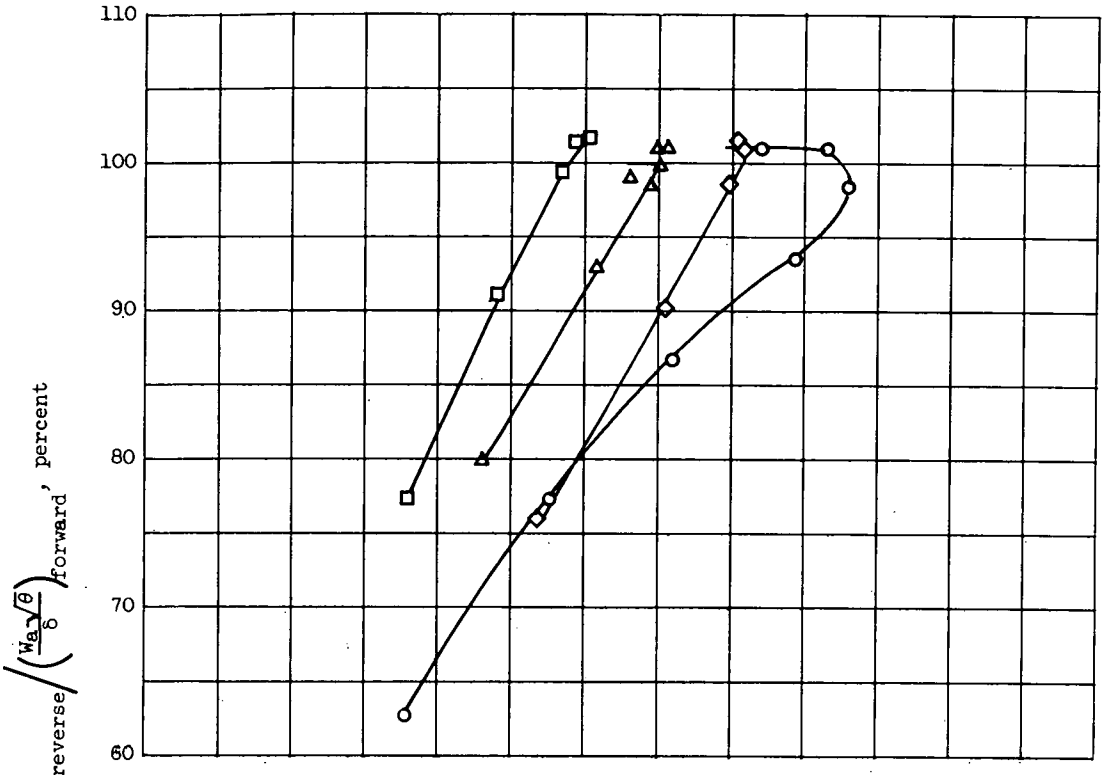

(c) Closed and filleted end configurations.

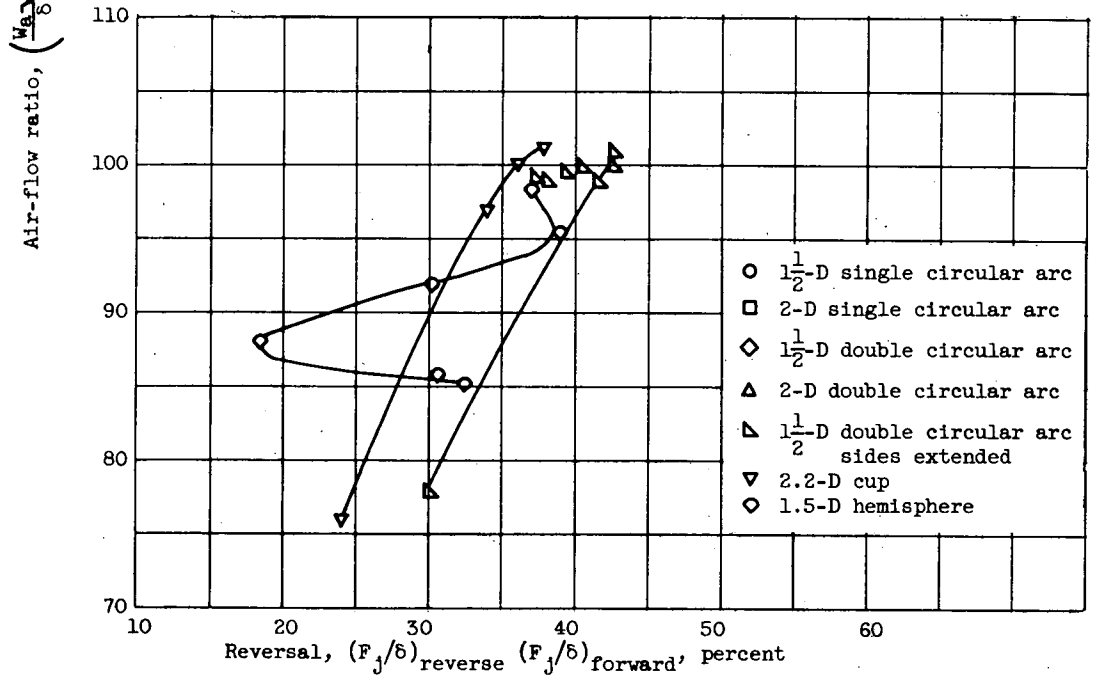

(d) Miscellaneous configurations.

Figure 5. - Concluded. Variation of corrected air flow with thrust reversal for various deflectors. Exhaust-nozzle pressure ratio, P_n/p_0, 2.0.

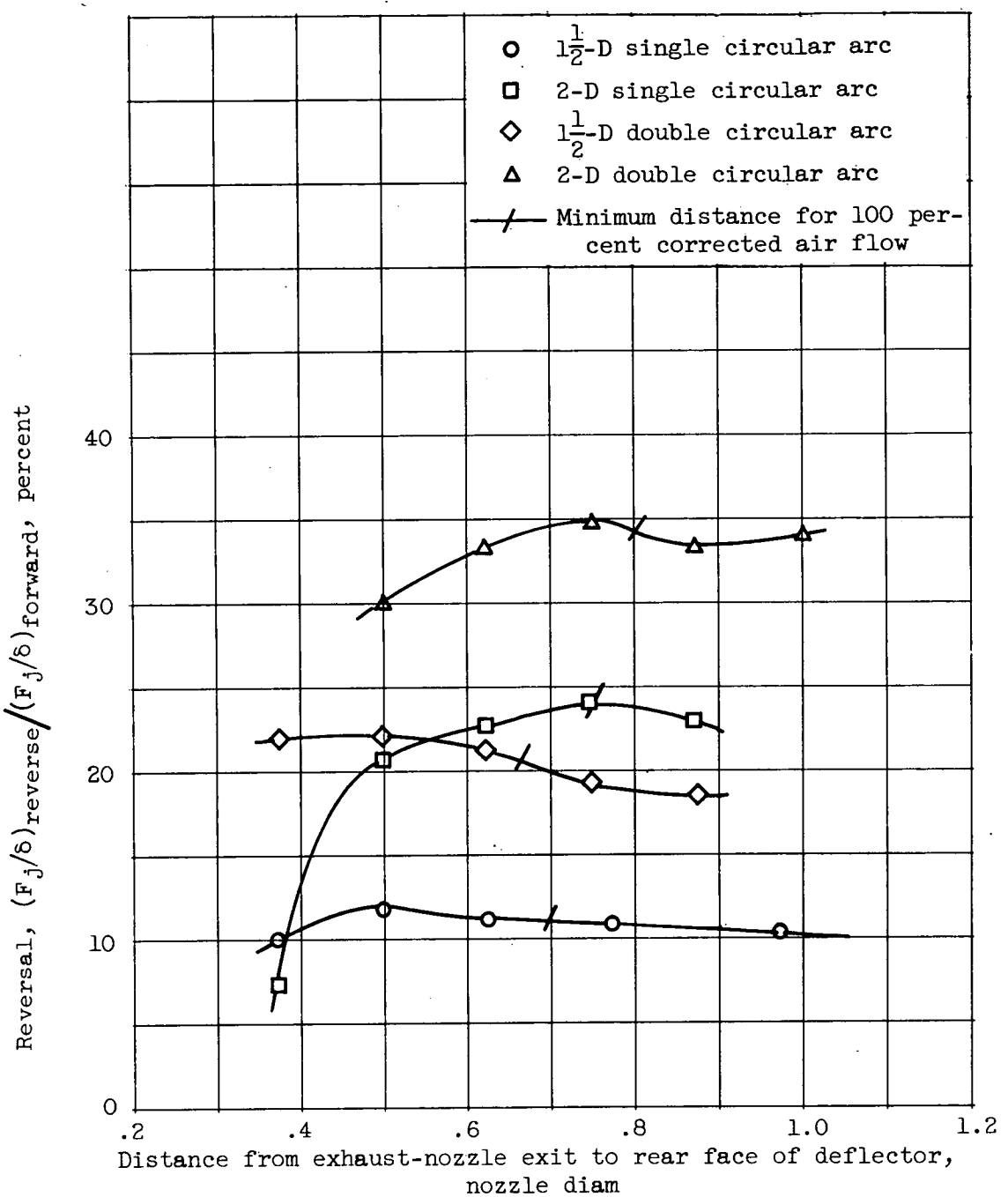

(a) Open-end configurations.

Figure 6. - Variation of thrust reversal with deflector spacing.

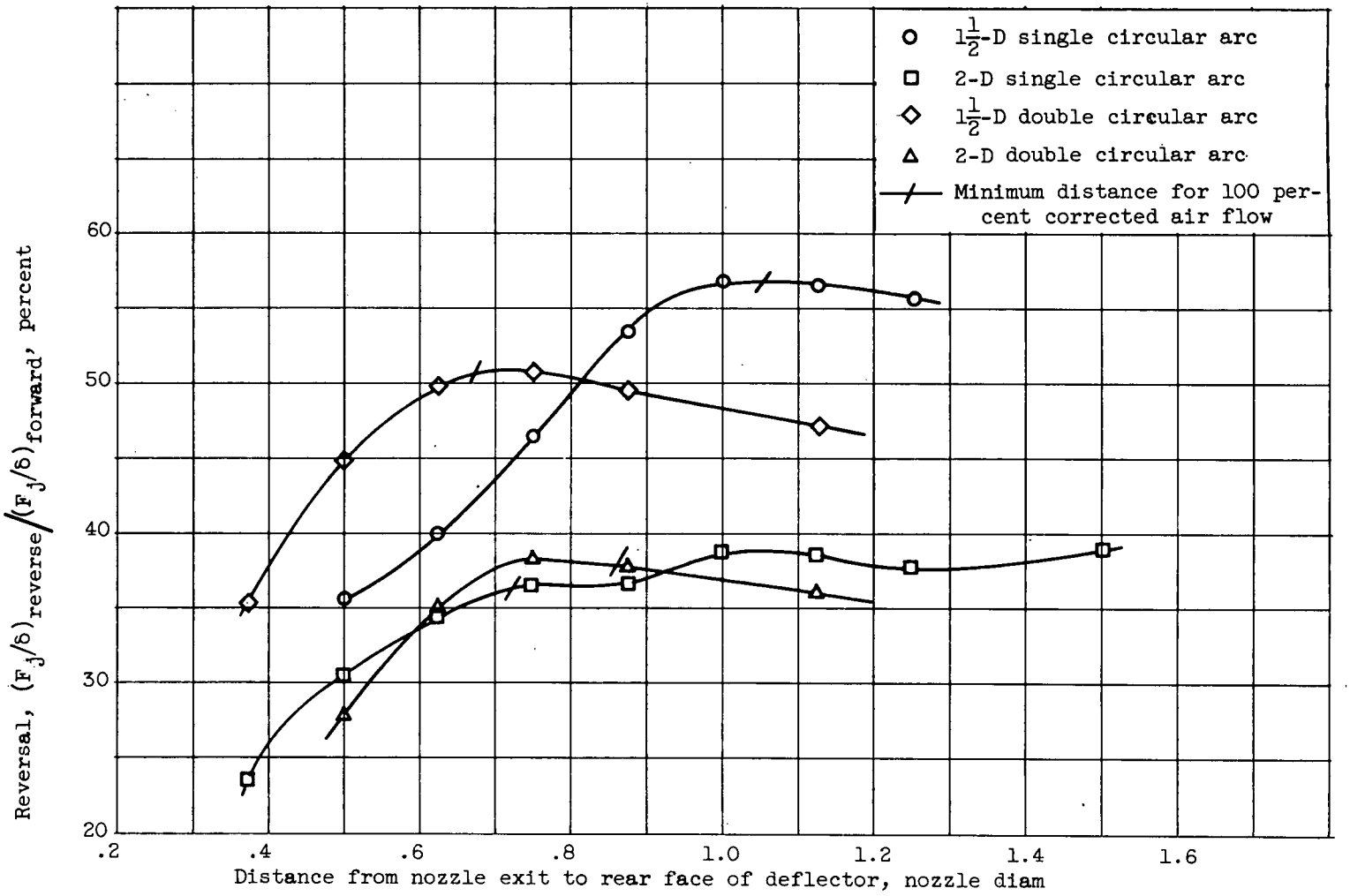

(b) Closed-end configurations.

Figure 6. - Continued. Variation of thrust reversal with deflector spacing.

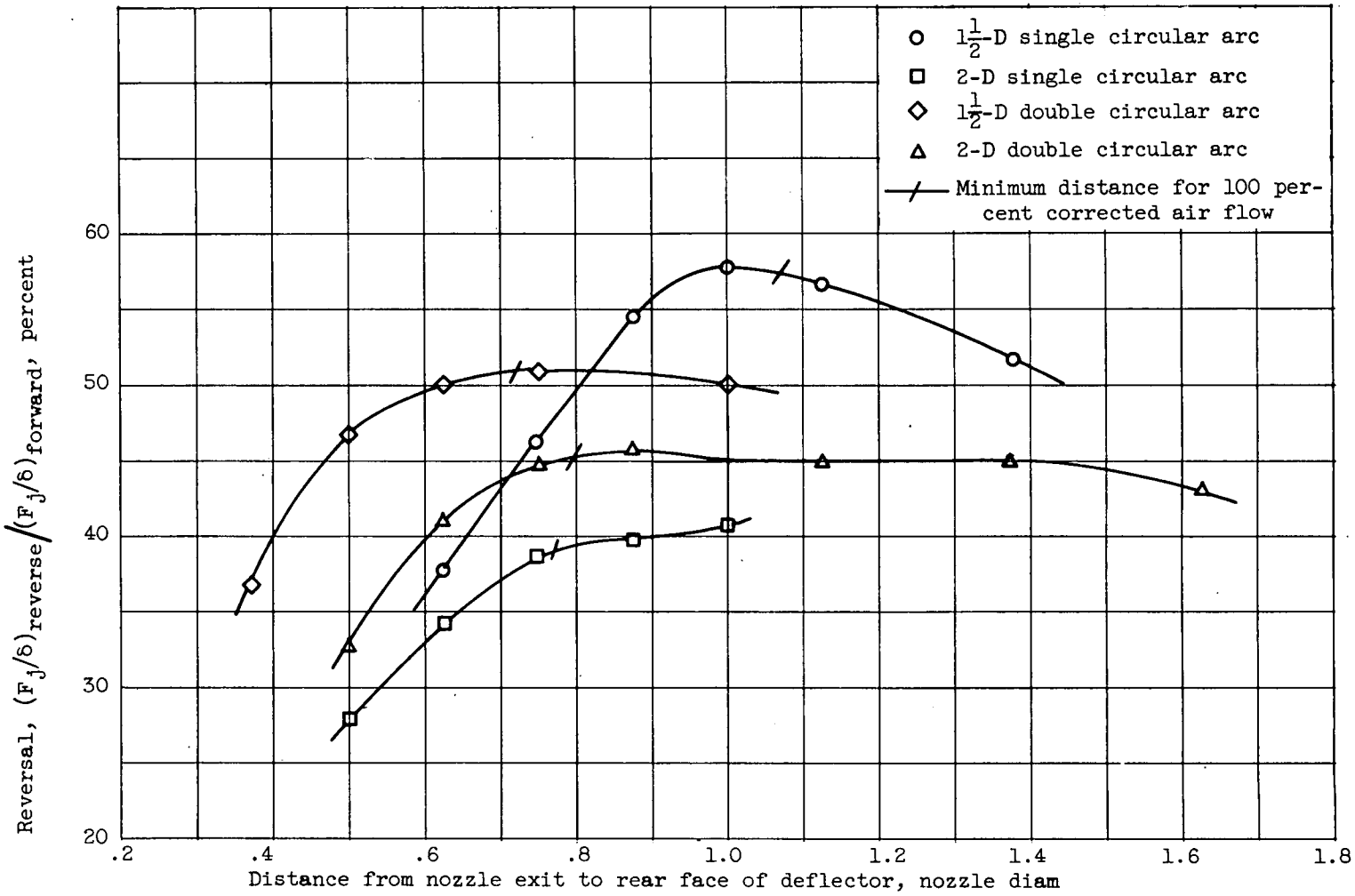

(c) Closed and filleted end configurations.

Figure 6. - Continued. Variation of thrust reversal with deflector spacing.

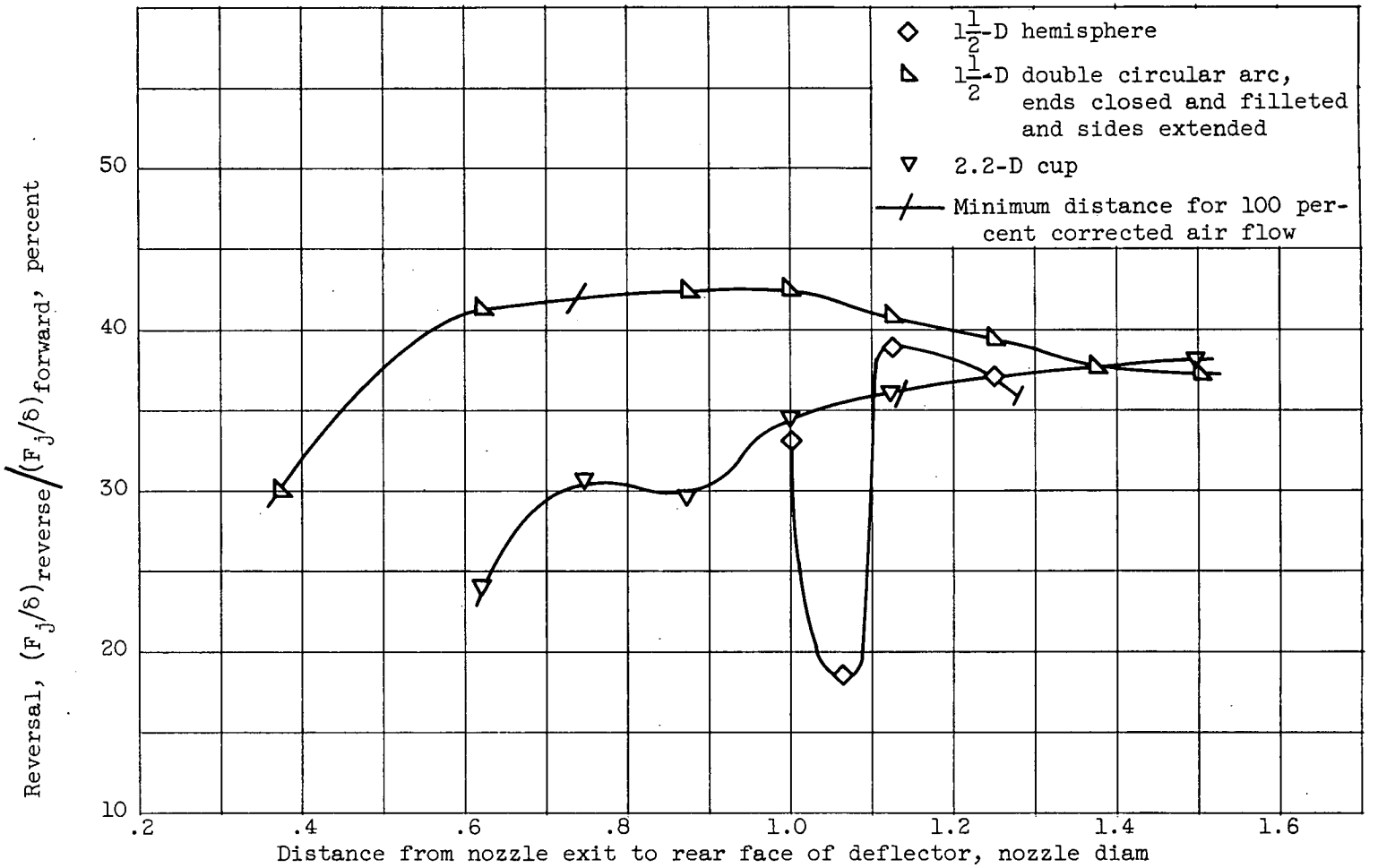

(d) Additional configurations.

Figure 6. - Concluded. Variation of thrust reversal with deflector spacing.

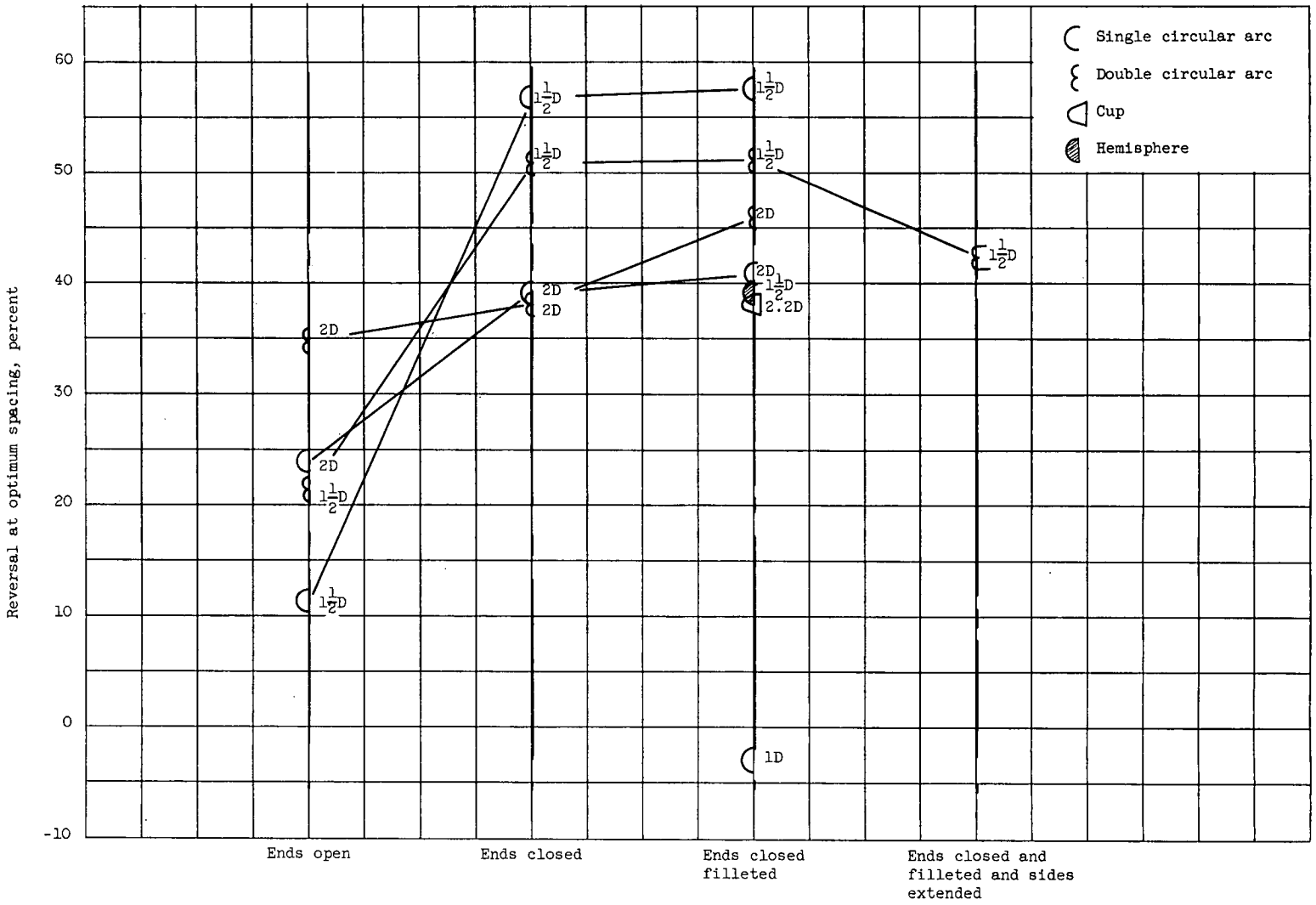

Figure 7. - Comparison of reverse thrusts obtained with various deflectors at optimum spacing and effects of modifications to basic configurations. Nozzle pressure ratio, P_n/p_0, 2.0.

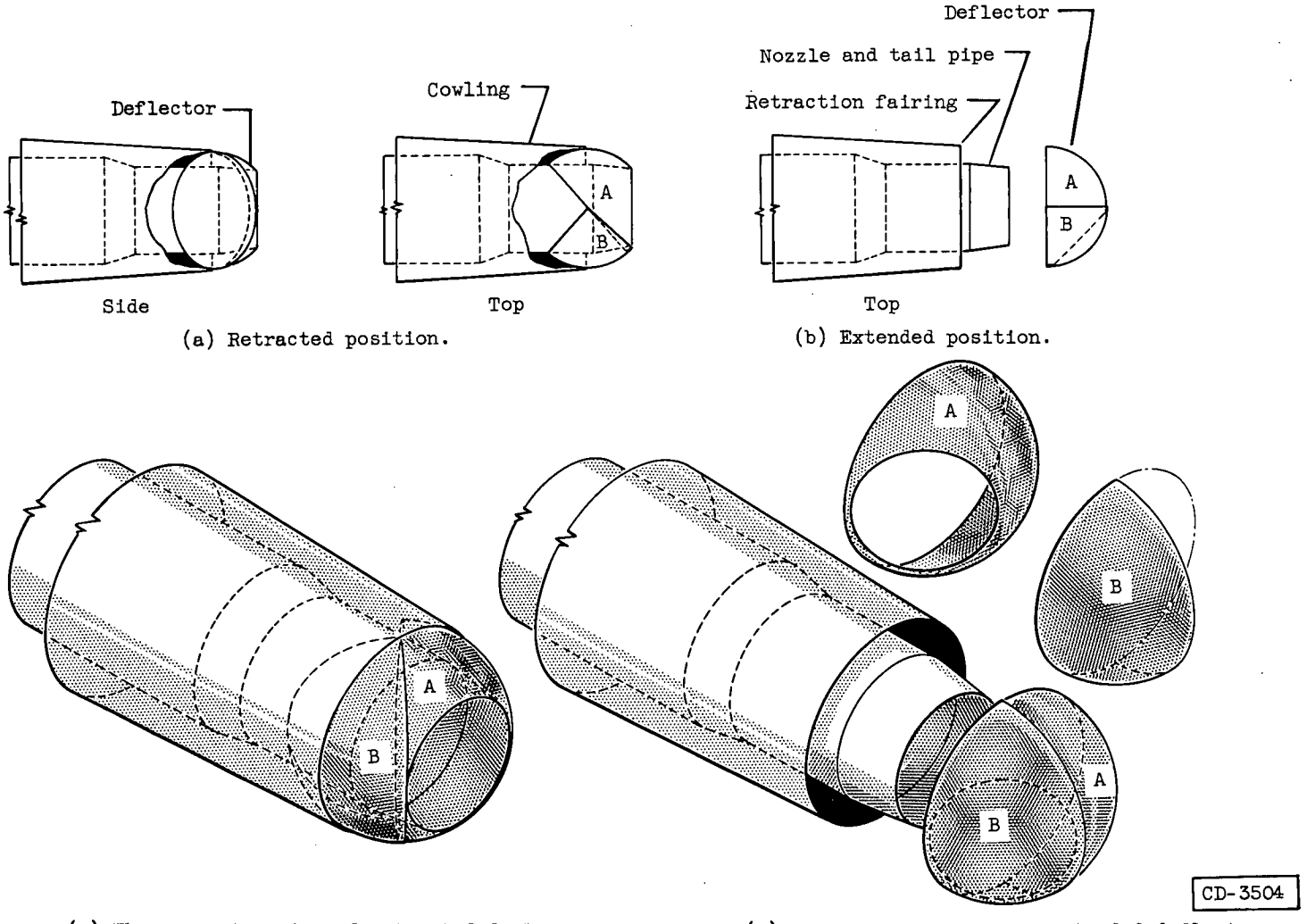

Figure 8. - Proposed method for retracting hemispherical deflector as installed on typical tail-pipe and cowling assembly.

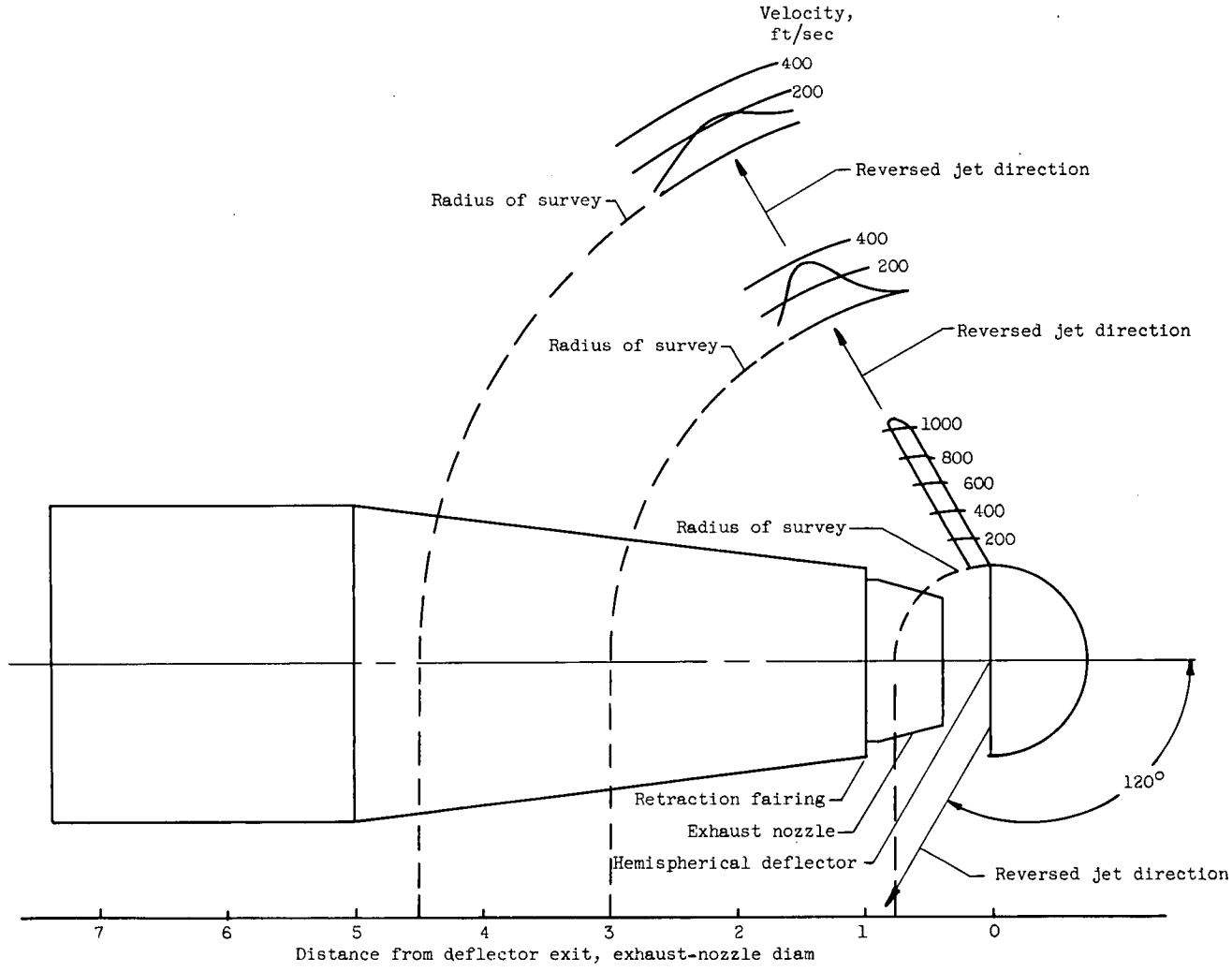

(a) Configuration P.

Figure 9. - Direction and magnitude of reversed jet flowing from hemispherical deflectors mounted on model tailpipe and cowling assembly.

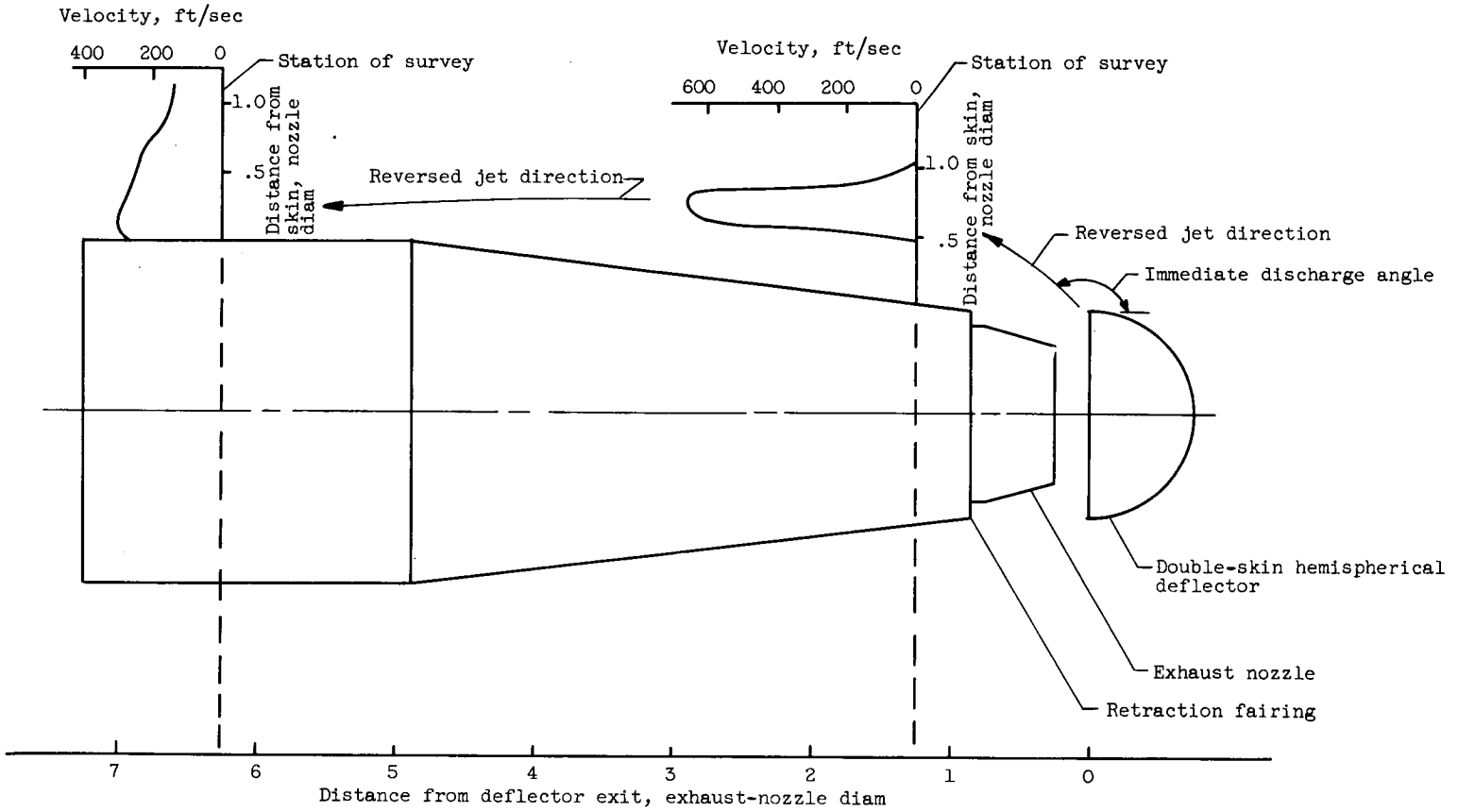

(b) Configuration Q.

Figure 9. - Concluded. Direction and magnitude of reversed jet flowing from hemispherical deflectors mounted on model tail-pipe and cowling assembly.

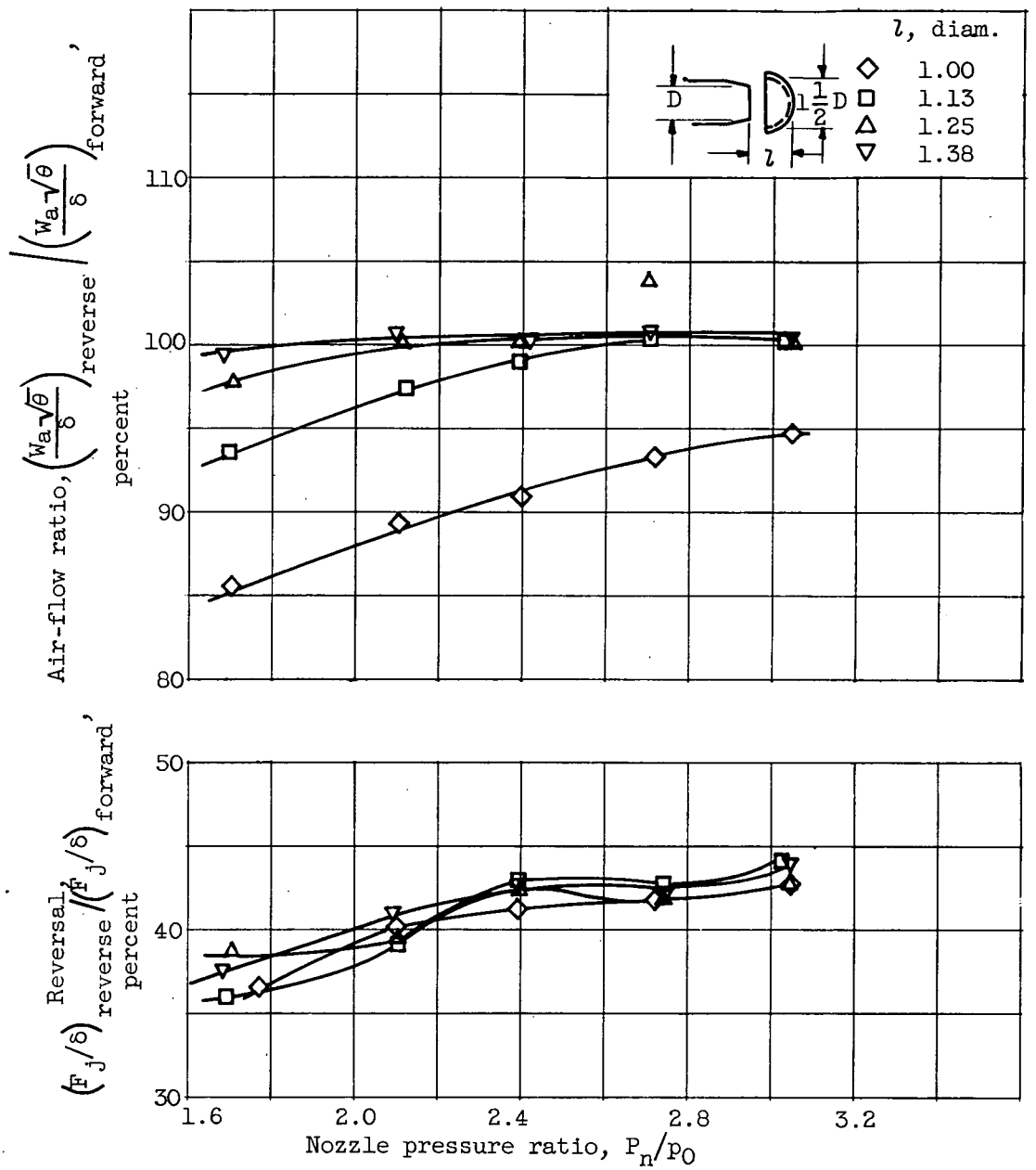

Figure 10. - Air-flow and thrust-reversal characteristics of double-skin hemisphere deflector over range of exhaust-nozzle pressure ratios.